Electronic Supplementary Material (ESI) for Dalton Transactions.

Supporting Information

Photochemically Generated Reactive Sites at Ruthenium/Gallium Complexes: Catalysis vs. Cluster Growth.

Raphael Bühler[#a], Maximilian Muhr[#a], Johannes Stephan [a], Robert Wolf [a], Max Schütz [a], Christian Gemel [a], Roland A. Fischer *[a]

a) Chair of Inorganic and Metalorganic Chemistry, Department of Chemistry, TUM School of Natural Sciences, Technical University Munich, Lichtenbergstraße 4, D-85748 Garching, Germany and Catalysis Research Center, Ernst-Otto-Fischer-Straße 1, D-85748 Garching, Germany.

Email: roland.fischer@tum.de

[#]M.M. and R.B. equally contributed to this work

Table of Contents

Crystallographic Data 3

NMR spectra 7

LIFDI mass spectra 21

IR spectra 30

UV-Vis spectra 31

Crystallographic Data

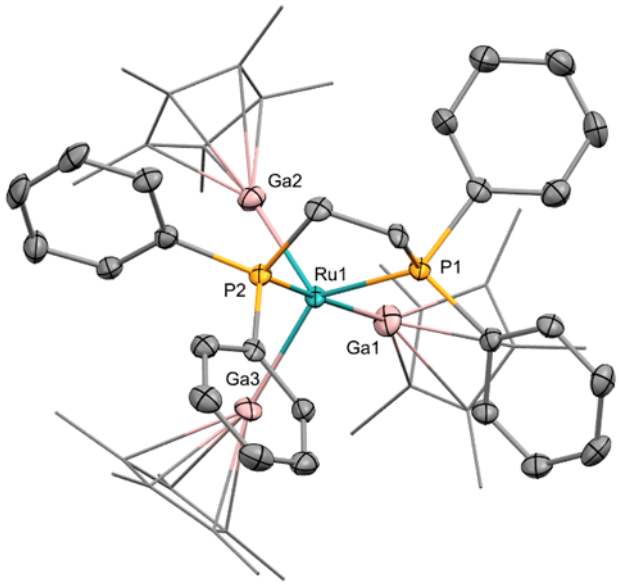

Figure S1: Crystal structure of [(dppe)Ru(GaCp)$_3$]. Co-crystallized molecule n-hexane and hydrogen atoms omitted for clarity. Ellipsoids drawn at 50% probability. Cp* in wireframes.*

*Table S1: Crystallographic data table for compound **4**.*

Chemical formula	$C_{62}H_{83}Ga_3P_2Ru$	
Formula weight	1200.45	
Temperature	100(2) K	
Wavelength	0.71073 Å	
Crystal size	0.059 x 0.066 x 0.225 mm	
Crystal habit	red-orange fragment	
Crystal system	monoclinic	
Space group	P 1 21/n 1	
Unit cell dimensions	a = 19.841(3) Å	α = 90°
	b = 12.724(2) Å	β = 99.625(7)°
	c = 22.940(4) Å	γ = 90°
Volume	5709.8(16) Å^3	
Z	4	
Density (calculated)	1.397 g/cm^3	
Absorption coefficient	1.753 mm^{-1}	
F(000)	2488	
Diffractometer	Bruker D8 Venture	

Radiation source	TXS rotating anode, Mo	
Theta range for data collection	2.41 to 25.68°	
Index ranges	-24<=h<=24, -15<=k<=15, -27<=l<=27	
Reflections collected	226471	
Indepedent reflections	10838 [R(int) = 0.1954]	
Coverage of independent reflections	99.9%	
Absorption correction	Multi-Scan	
Structure solution technique	direct methods	
Structure solution program	SHELXT 2014/5 (Sheldrick, 2014)	
Refinement method	Full-matrix least-squares on F^2	
Refinement program	SHELXL-2018/3 (Sheldrick, 2018)	
Function minimized	$\Sigma\, w(F_o^2 - F_c^2)^2$	
Data / restraints / parameters	10838 / 0 / 630	
Goodness-of-fit on F^2	1.021	
Δ/σ_{max}	0.001	
Final R indices	6979 data; I>2σ(I)	R1 = 0.0496,
	all data	wR2 = 0.0861
		R1 = 0.1073,
		wR2 = 0.1037
Weighting scheme	$w=1/[\sigma^2(F_o^2)+(0.0318P)^2+16.8706P]$	
	where $P=(F_o^2+2F_c^2)/3$	
Largest diff. peak and hole	0.982 and -0.774 eÅ^{-3}	
R.M.S. deviation from mean	0.114 eÅ^{-3}	

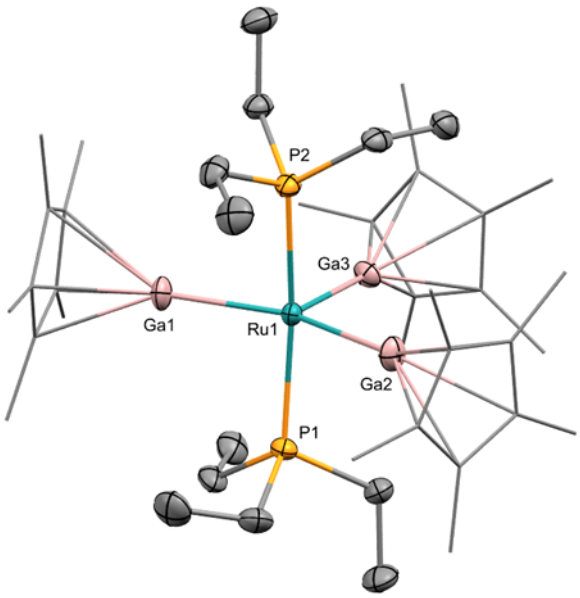

Figure S2: Crystal structure of [$(Et_3P)_2Ru(GaCp^*)_3$]. Co-crystallized molecule n-hexane and hydrogen atoms omitted for clarity. Ellipsoids drawn at 50% probability. Cp in wireframes.*

Table S2: Crystallographic data table for compound [$Ru(GaCp^*)_3(PEt_3)_2$].

Chemical formula	$C_{48}H_{88.07}Ga_3P_2Ru$	
Formula weight	1037.42	
Temperature	123(2) K	
Wavelength	0.71073 Å	
Crystal size	0.238 x 0.321 x 0.374 mm	
Crystal habit	orange block	
Crystal system	orthorhombic	
Space group	P 21 21 21	
Unit cell dimensions	a = 12.268(4) Å	α = 90°
	b = 19.291(7) Å	β = 90°
	c = 21.580(6) Å	γ = 90°
Volume	5107.(3) Å3	
Z	4	
Density (calculated)	1.349 g/cm^3	
Absorption coefficient	1.948 mm^{-1}	
F(000)	2172	
Diffractometer	Bruker D8 Venture	
Radiation source	TXS rotating anode, Mo	

Theta range for data collection	2.51 to 25.90°	
Index ranges	-14<=h<=15, -23<=k<=23, -26<=l<=26	
Reflections collected	137547	
Indepedent reflections	9855 [R(int) = 0.0279]	
Coverage of independent reflections	99.3%	
Absorption correction	Multi-Scan	
Structure solution technique	direct methods	
Structure solution program	SHELXT 2014/5 (Sheldrick, 2014)	
Refinement method	Full-matrix least-squares on F^2	
Refinement program	SHELXL-2019/1 (Sheldrick, 2019)	
Function minimized	$\Sigma\, w(F_o^2 - F_c^2)^2$	
Data / restraints / parameters	9855 / 101 / 531	
Goodness-of-fit on F^2	1.051	
Δ/σ_{max}	0.003	
Final R indices	9563 data; I>2σ(I)	R1 = 0.0172,
	all data	wR2 = 0.0451
		R1 = 0.0183,
		wR2 = 0.0455
Weighting scheme	$w=1/[\sigma^2(F_o^2)+(0.0257P)^2+1.6529P]$	
	where $P=(F_o^2+2F_c^2)/3$	
Largest diff. peak and hole	0.485 and -0.396 $eÅ^{-3}$	
R.M.S. deviation from mean	0.049 $eÅ^{-3}$	

NMR spectra

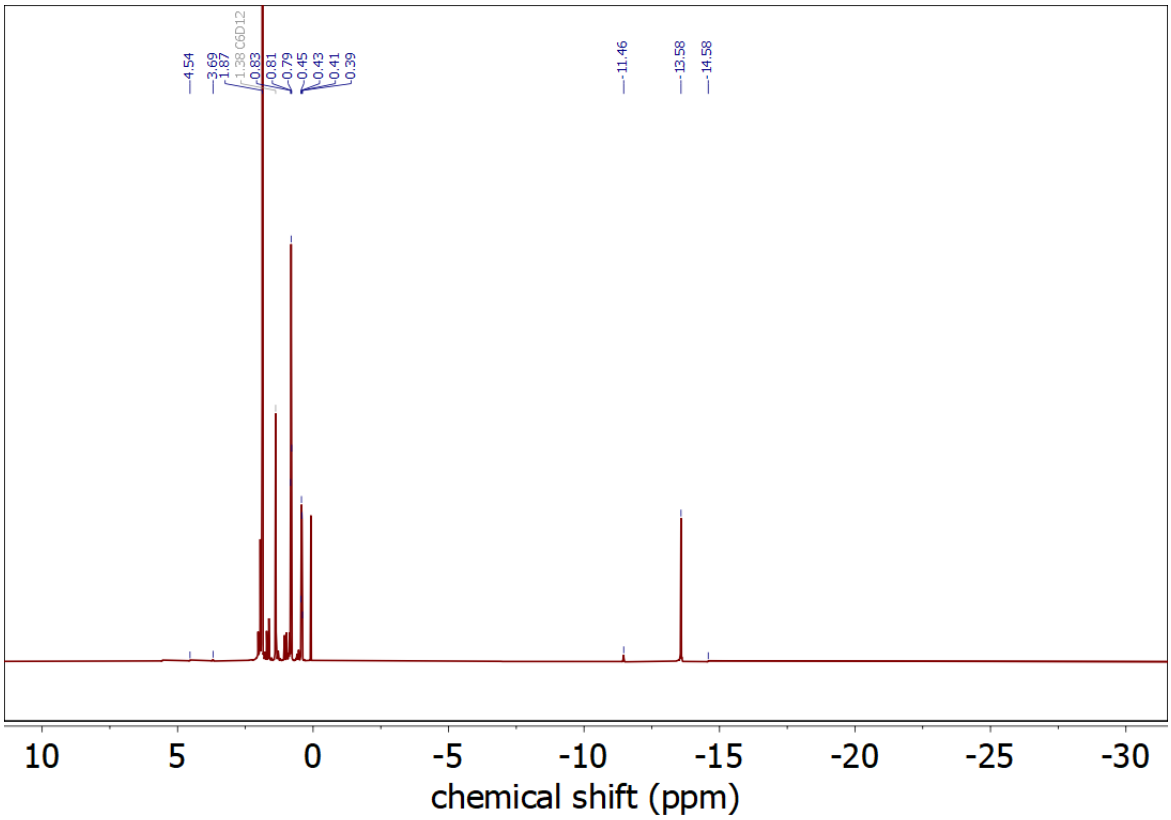

*Figure S3: ^{1}H NMR spectrum of **1** after 30 min irradiation at 350 nm in C_6D_{12}.*

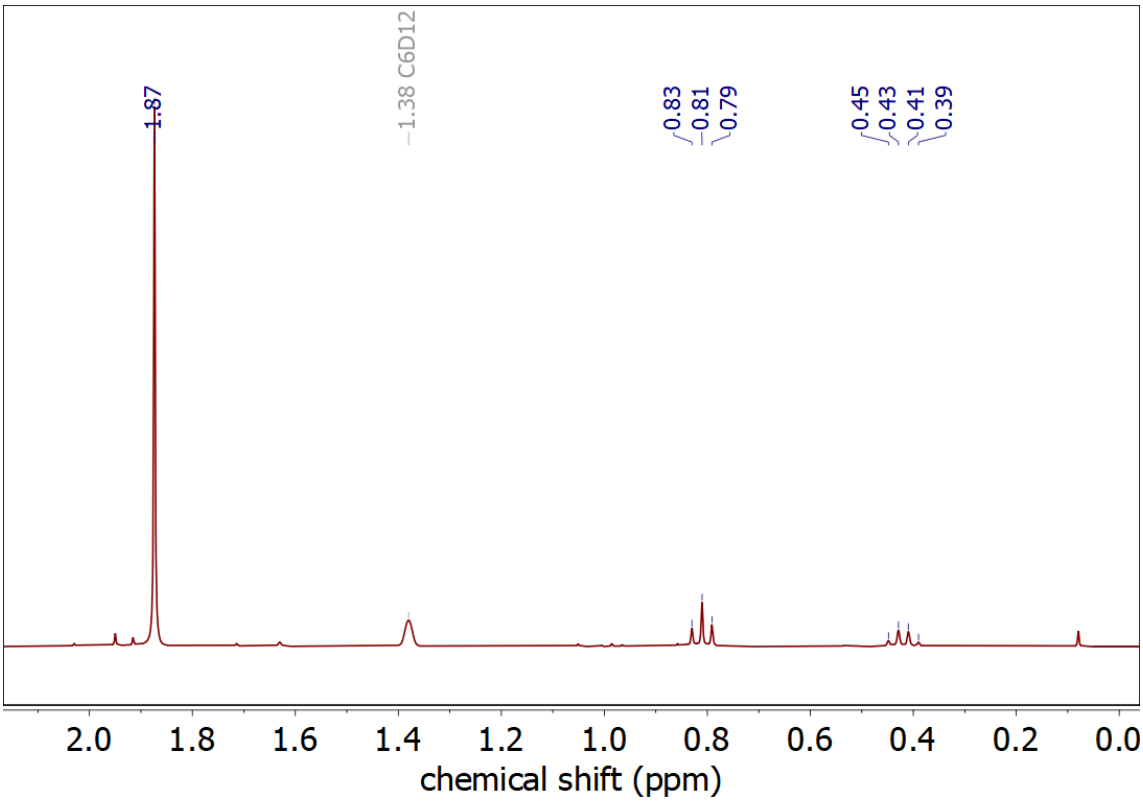

*Figure S4: ^{1}H NMR spectrum of **1** after 30 min irradiation at 350 nm in C_6D_{12}. Excerpt of the aliphatic range.*

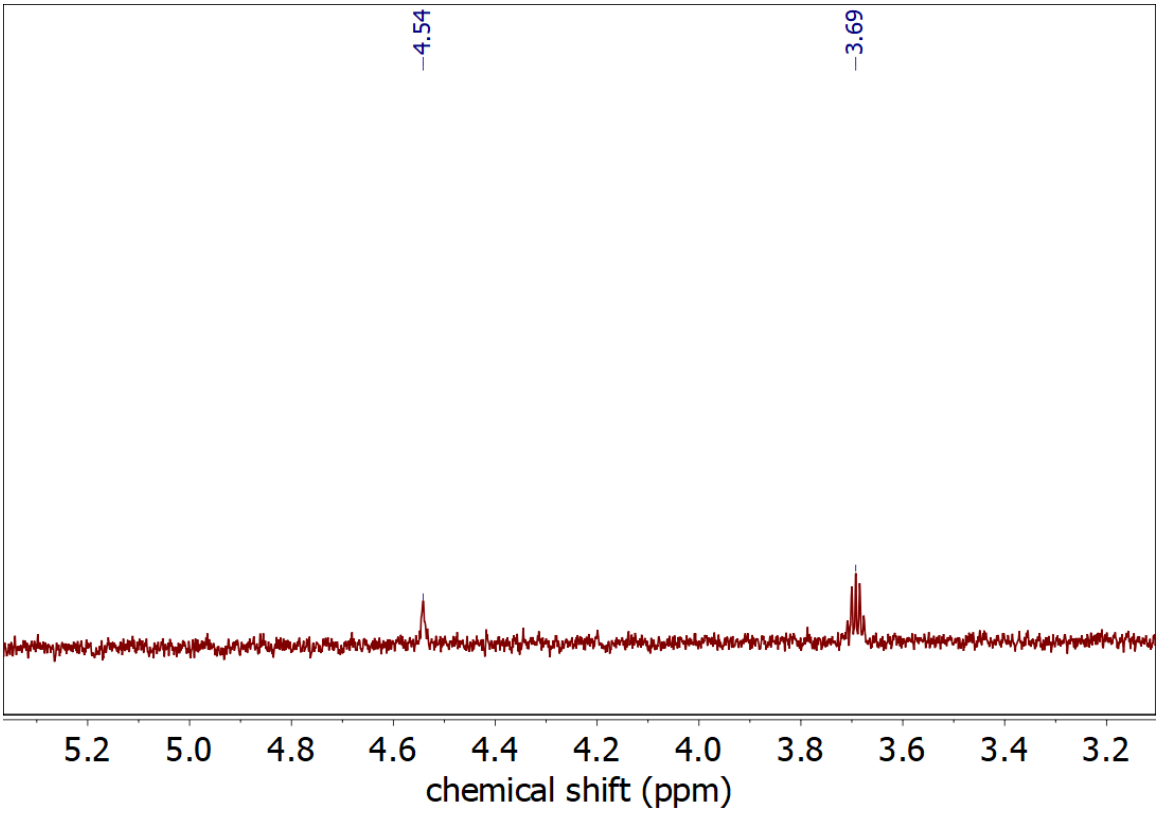

*Figure S5: ^{1}H NMR spectrum of **1** after 30 min irradiation at 350 nm in C_6D_{12}. Excerpt showing free hydrogen (4.54 ppm) and free triethylsilane (3.69 ppm, H-Si).*

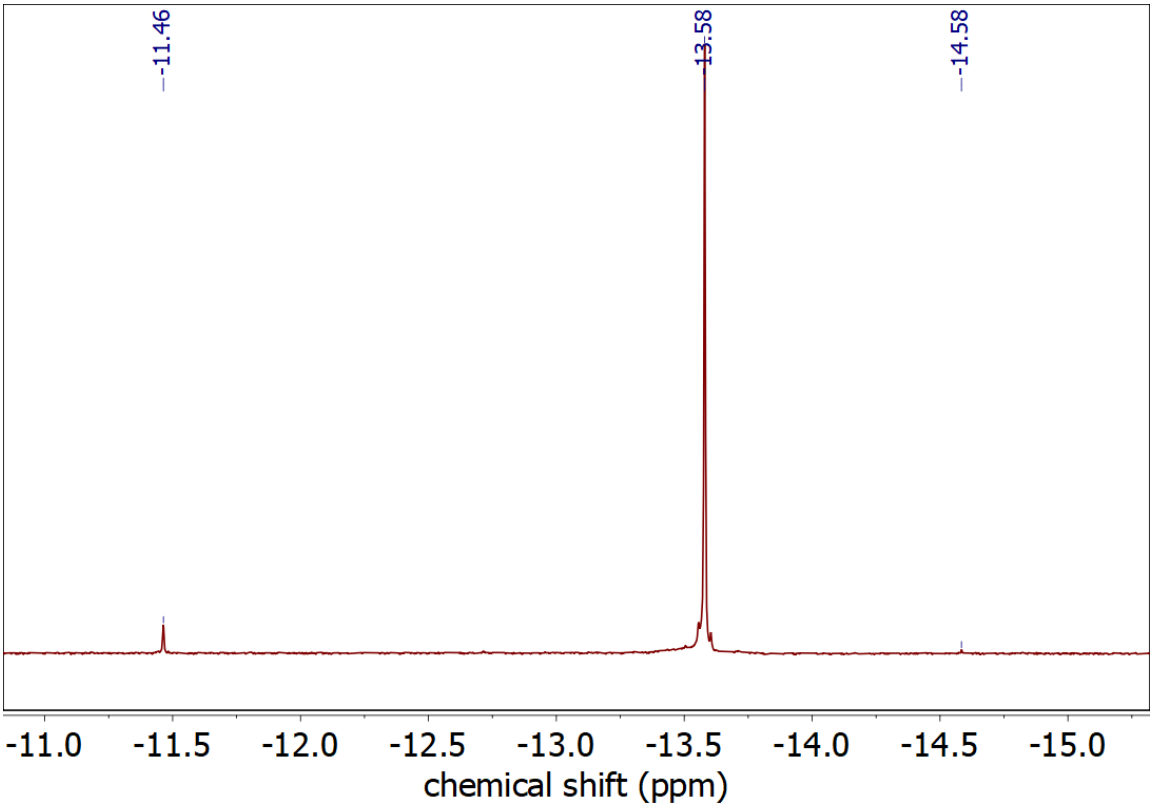

*Figure S6: ^{1}H NMR spectrum of **1** after 30 min irradiation at 350 nm in C_6D_{12}. Excerpt of the hydridic range, showing two new signals at -11.46 and -14.58 ppm.*

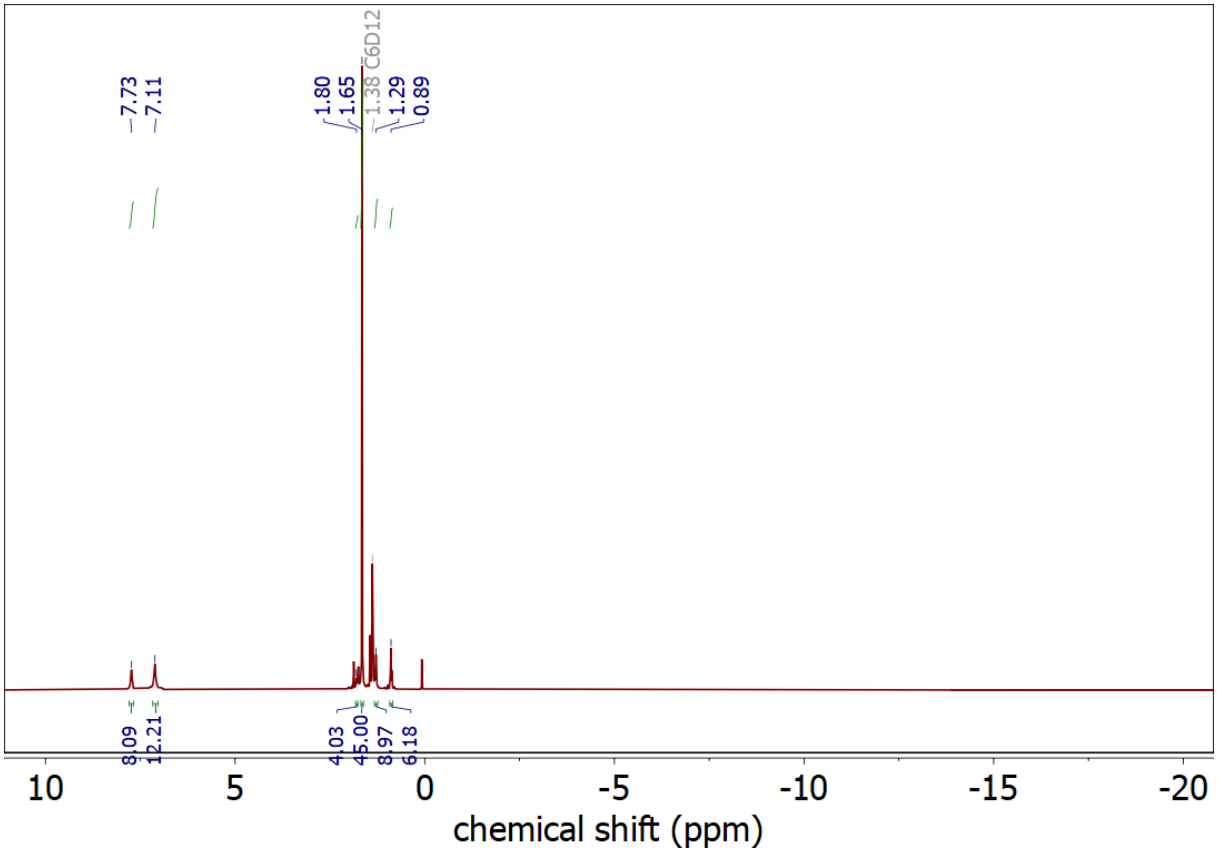

*Figure S7: Full range ^{1}H NMR of **4** in C_6D_{12}. No new hydride signals.*

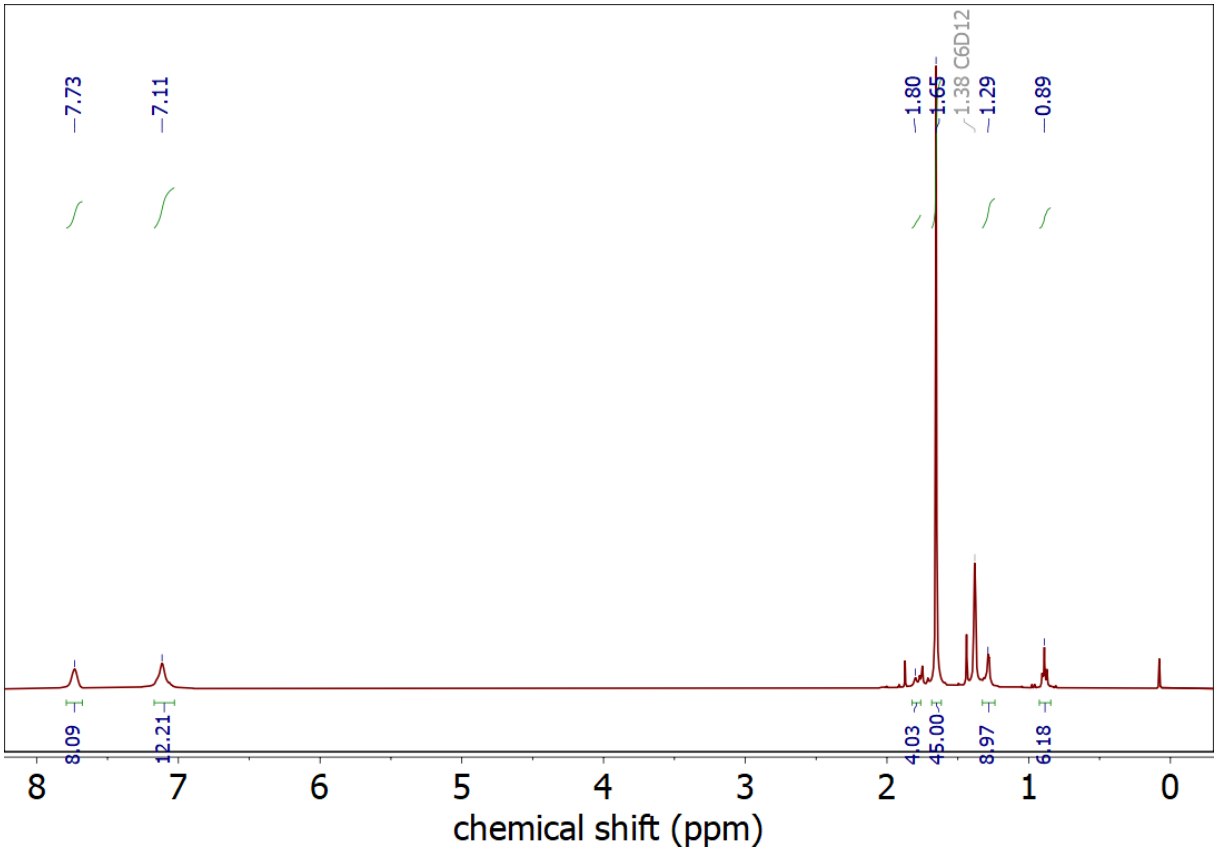

*Figure S8: Zoomed into ^{1}H NMR of **4** in C_6D_{12}.*

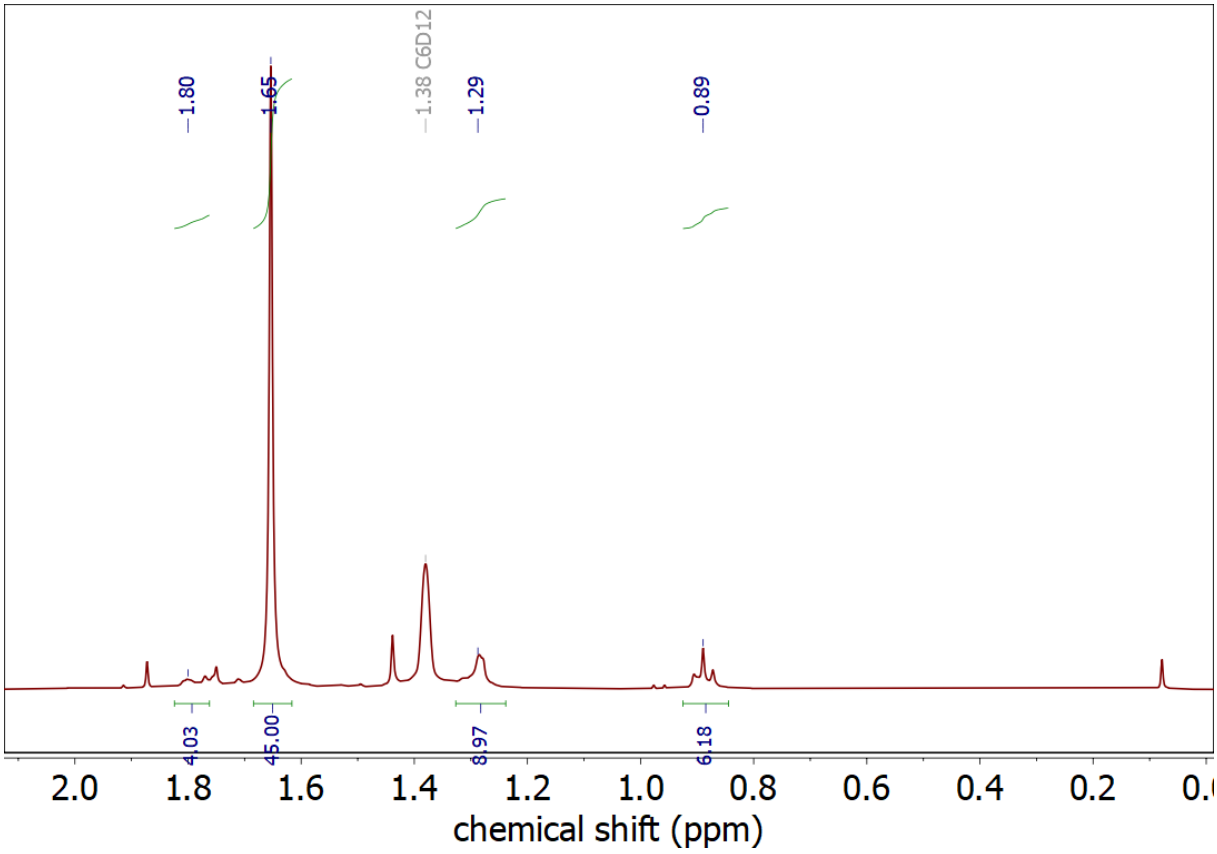

*Figure S9: Zoomed into ^{1}H NMR of **4** in C_6D_{12} – aliphatic range.*

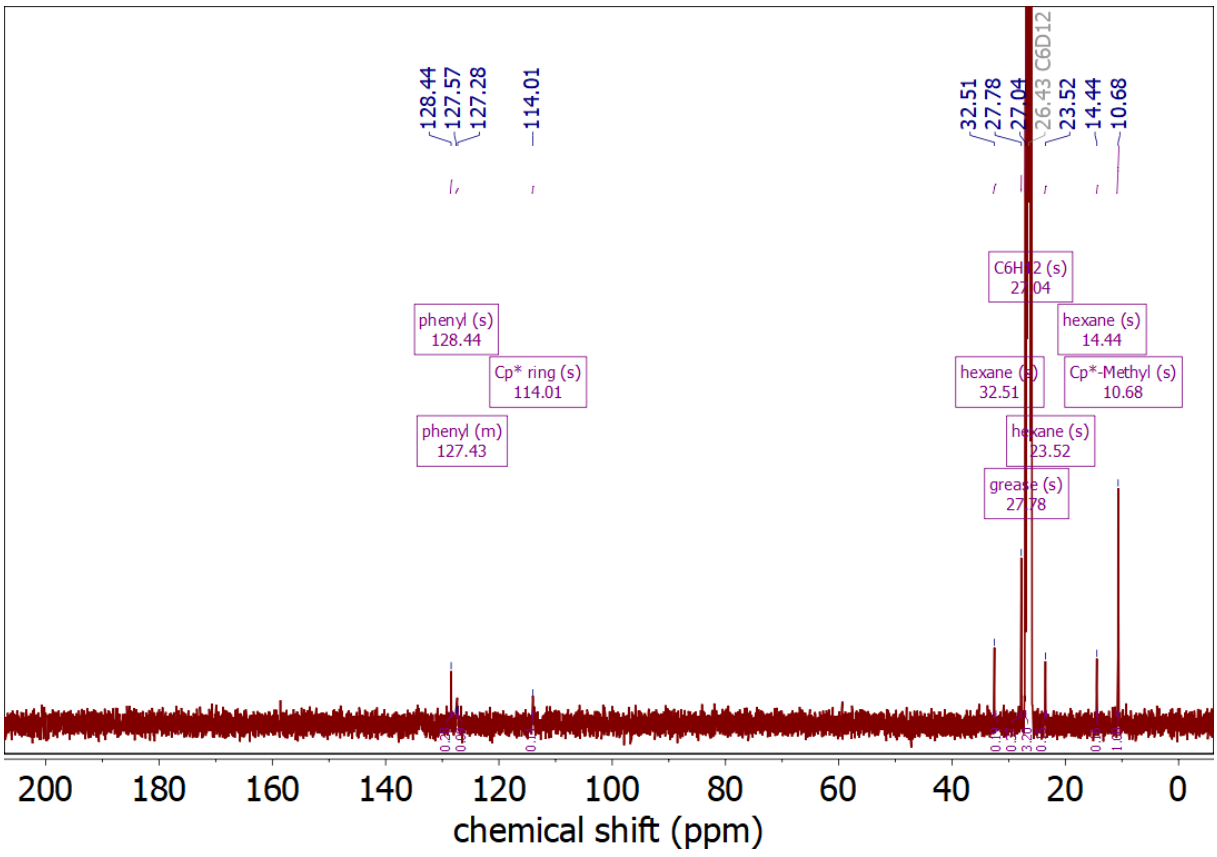

*Figure 10: SFull range ^{13}C NMR of **4** in C_6D_{12}.*

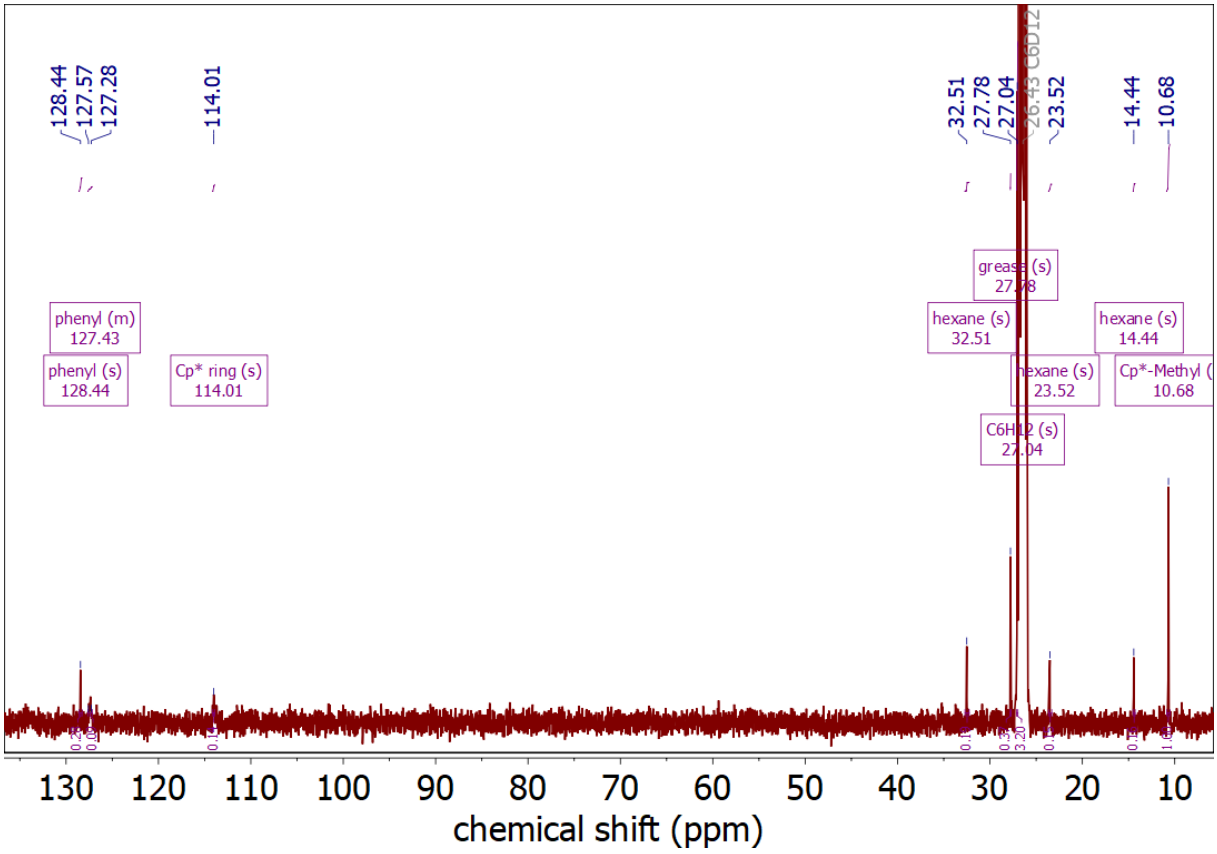

*Figure S11: Zoomed into ^{13}C NMR of **4** in C_6D_{12}.*

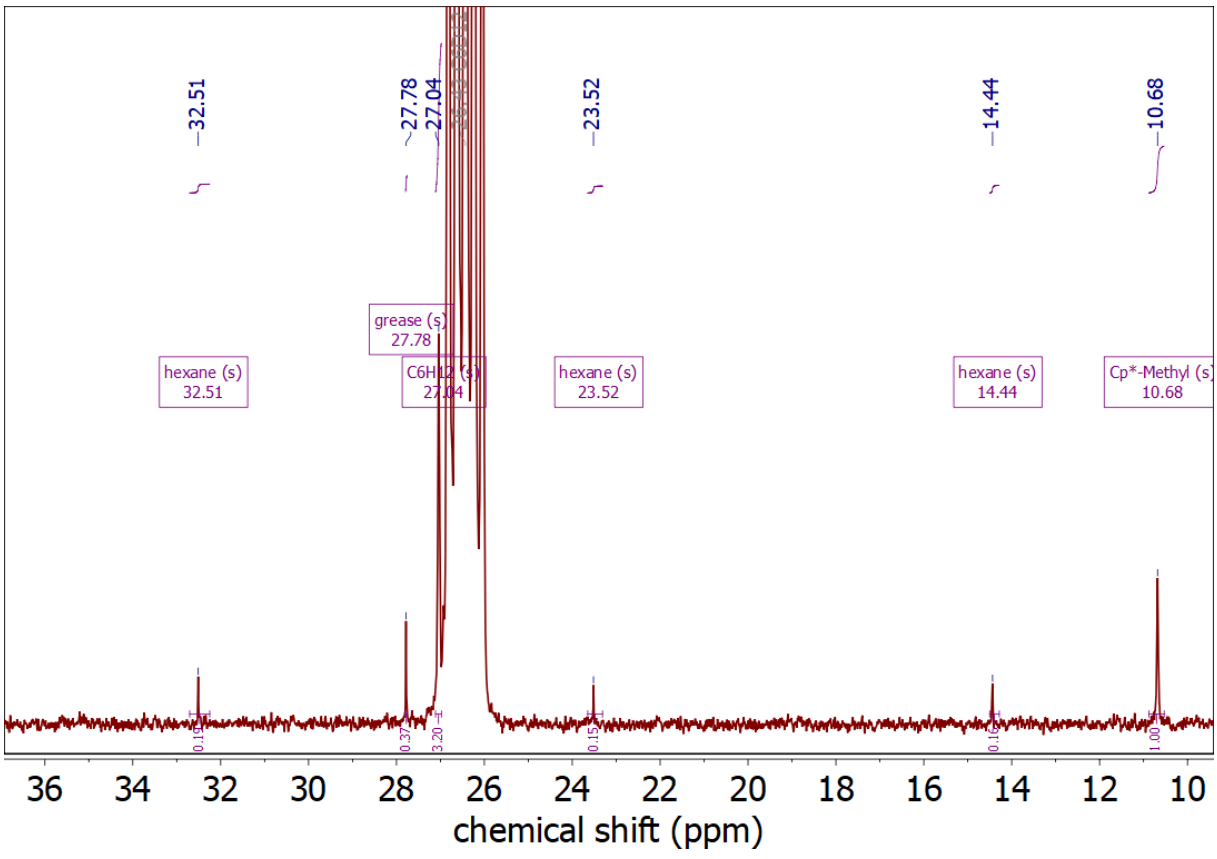

*Figure S12: ^{13}C NMR of **4** in C_6D_{12} – aliphatic range.*

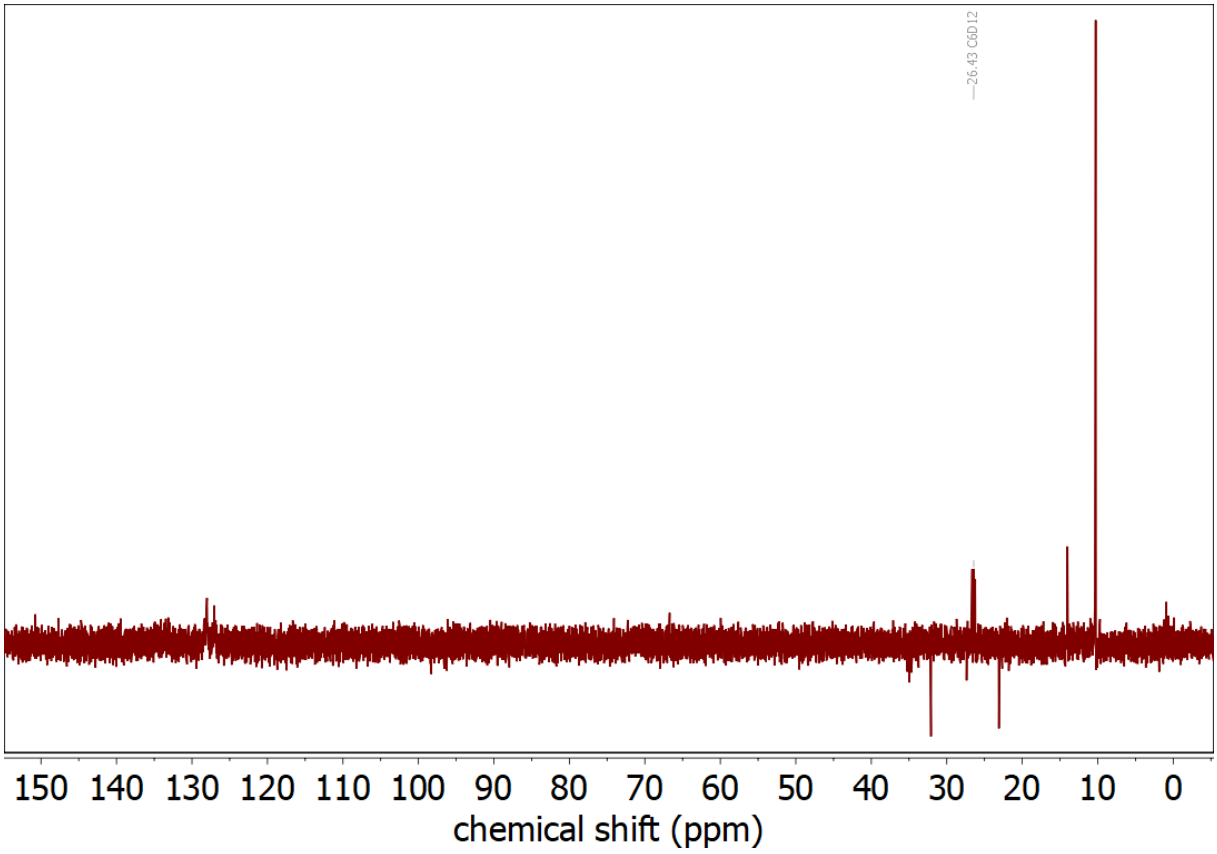

*Figure S13: Full range DEPT 135 of **4** in C_6D_{12}.*

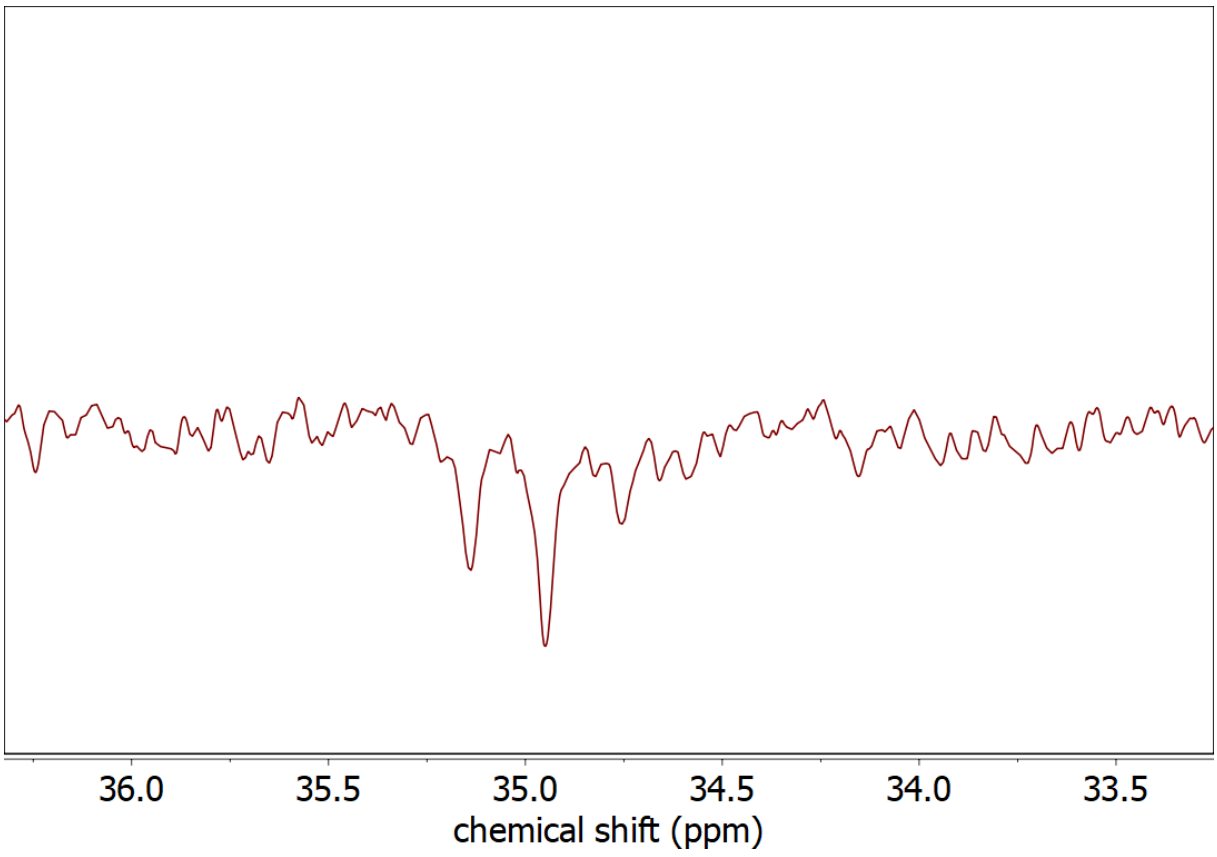

*Figure S14: Zoomed into DEPT 135 of **4** in C_6D_{12}. Negative ^{13}C triplet (due to ^{31}P coupling) of dppe H_2C-CH_2 bridge.*

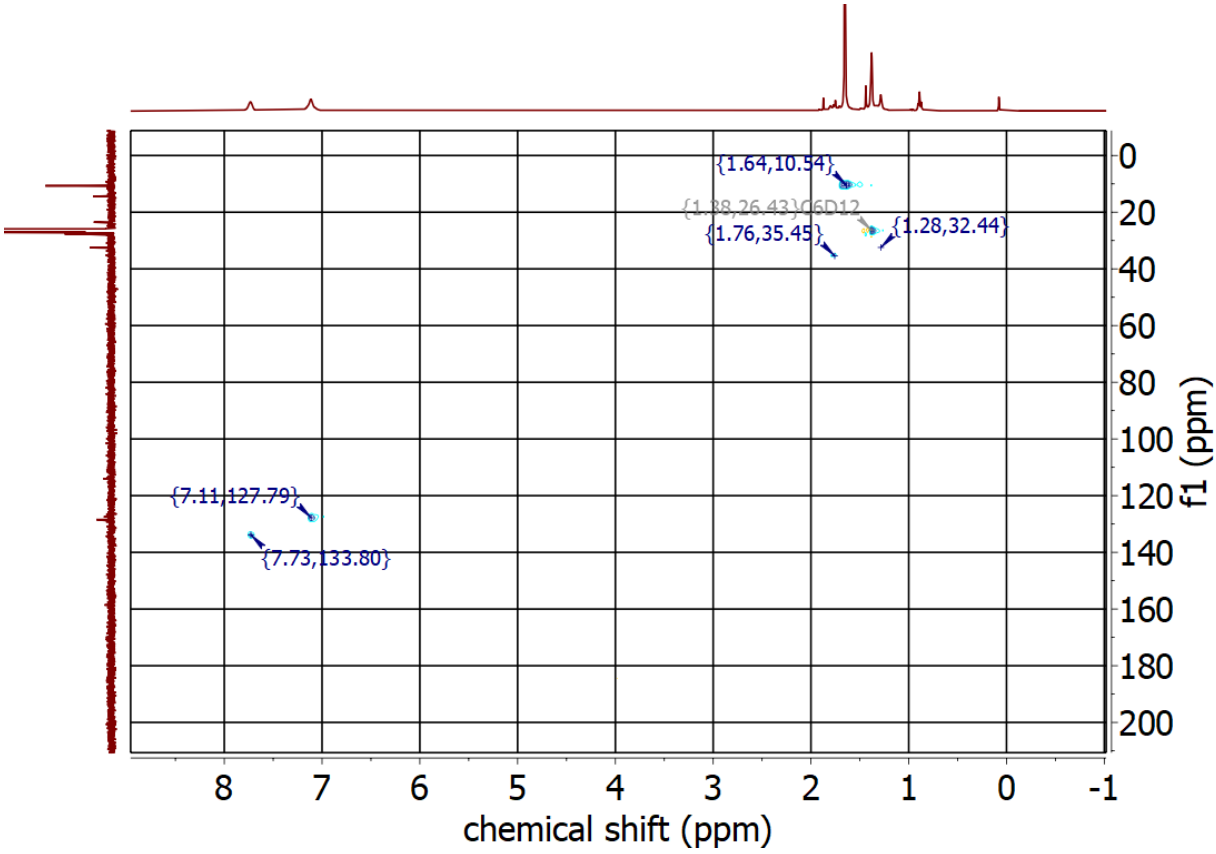

*Figure S15: Full range HSQC spectrum of **4** in C_6D_{12}.*

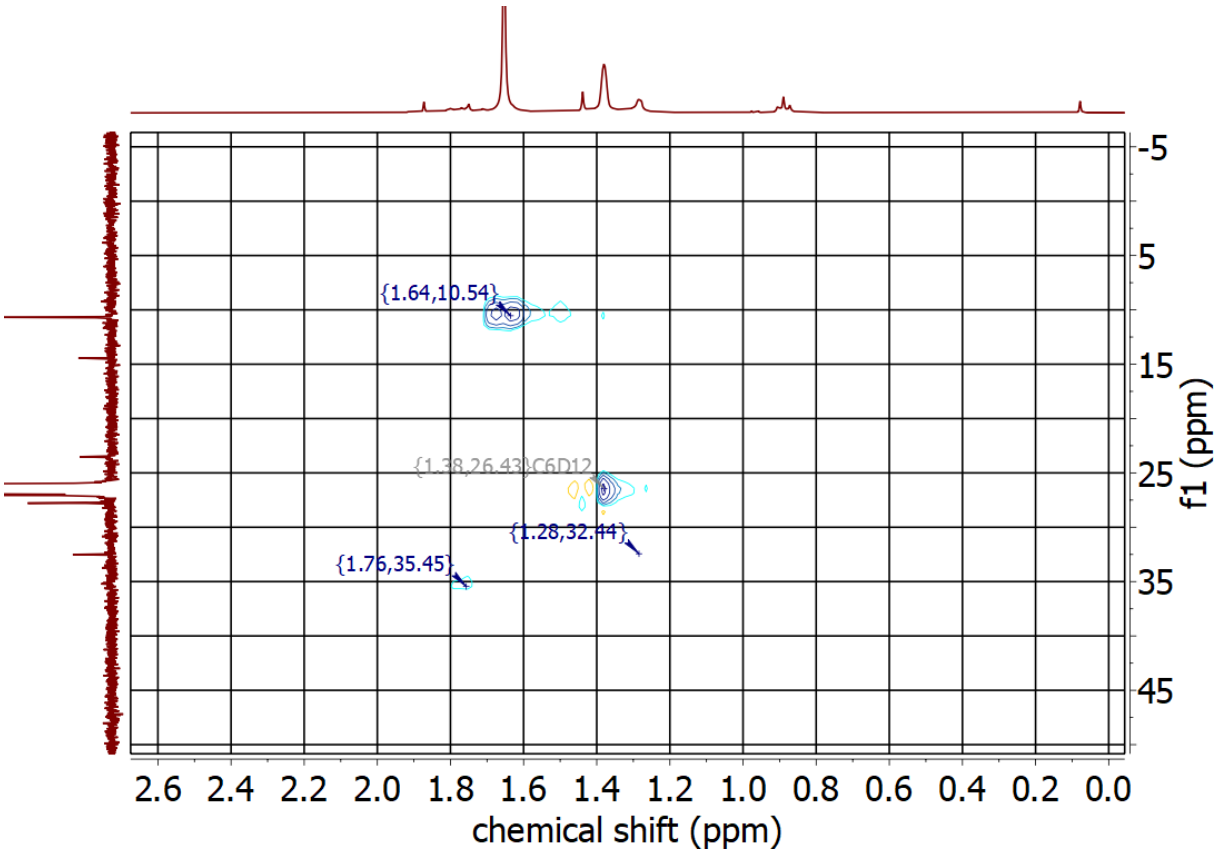

*Figure S16: HSQC spectrum of **4** in C_6D_{12} – aliphatic range.*

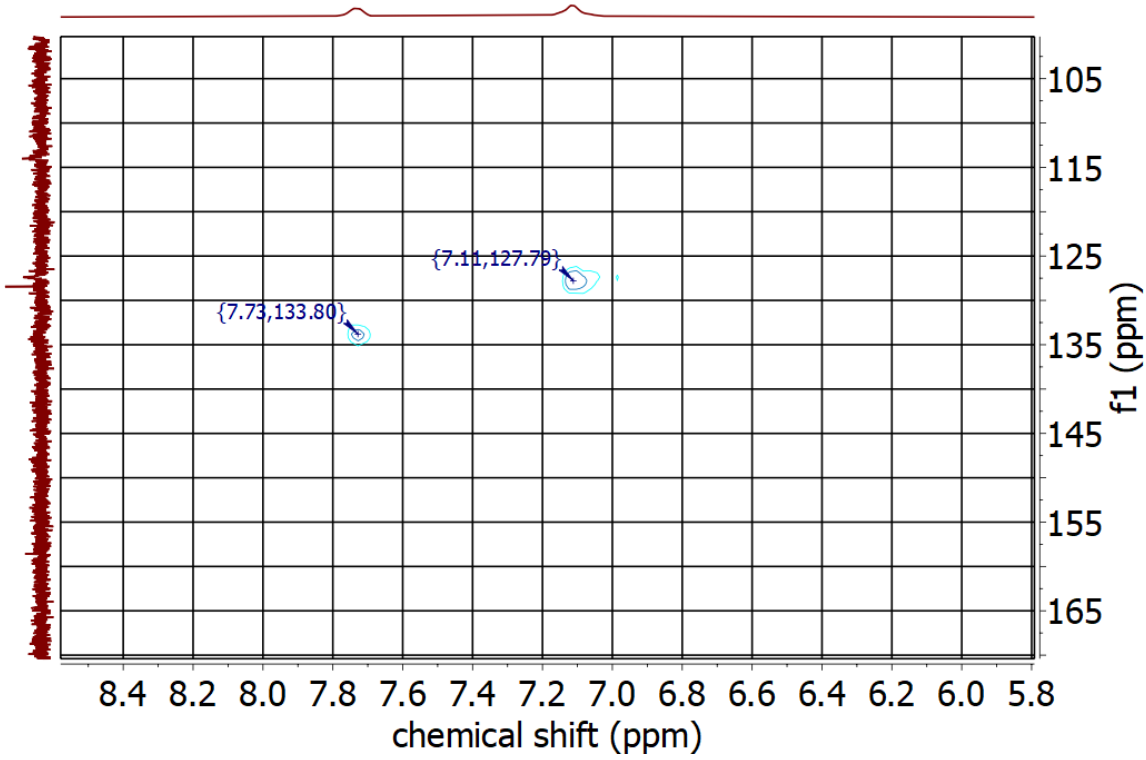

*Figure S17: HSQC spectrum of **4** in C_6D_{12} – aromatic range.*

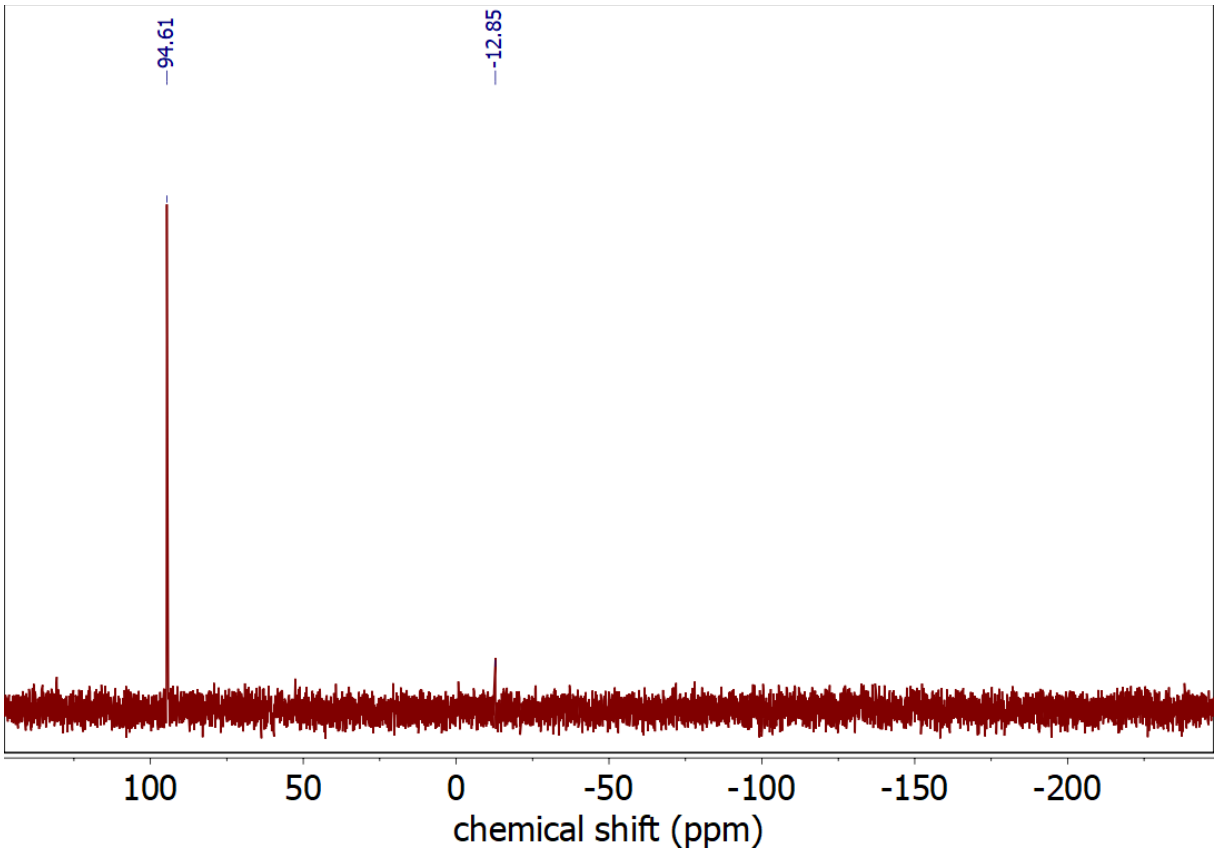

*Figure S18: Full range ^{31}P spectrum of **4** in C_6D_{12}.*

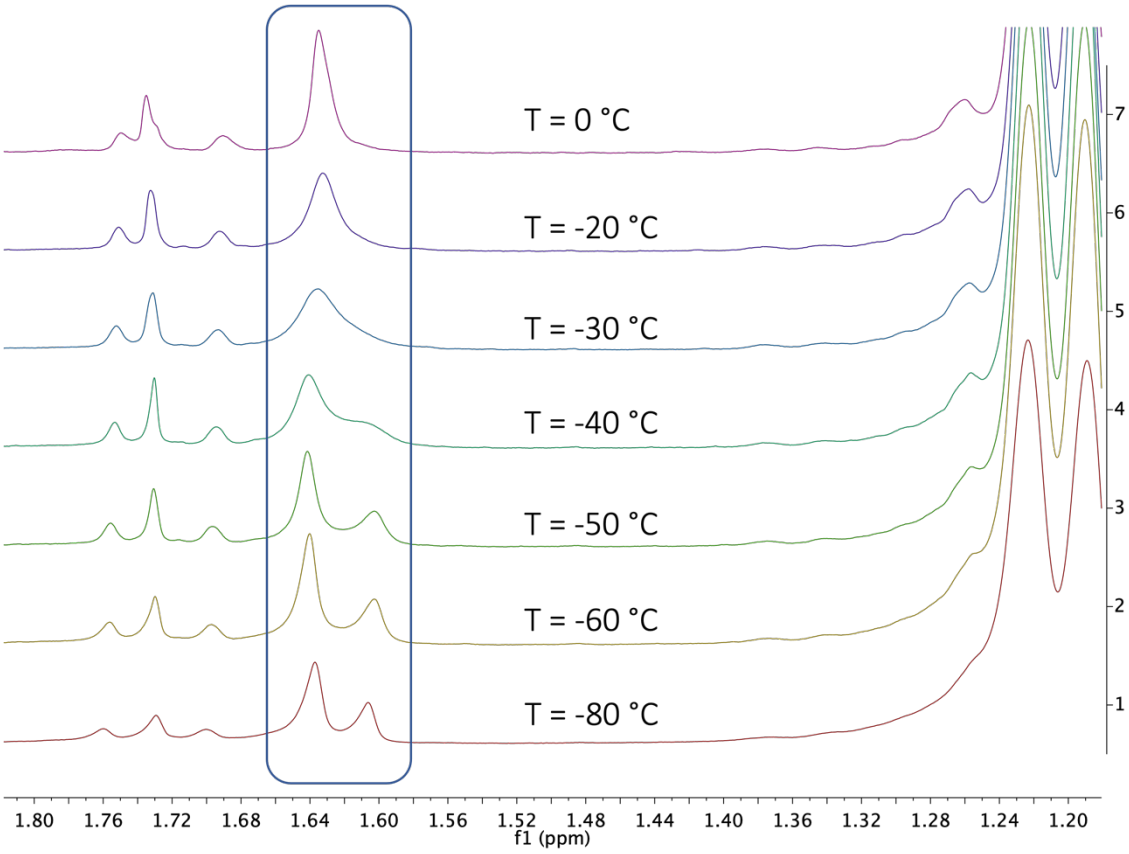

*Figure S19: Variable Temperature ^{1}H-NMR spectra of **4** between -80 and 0 °C in* n-hexane-d_{14}.

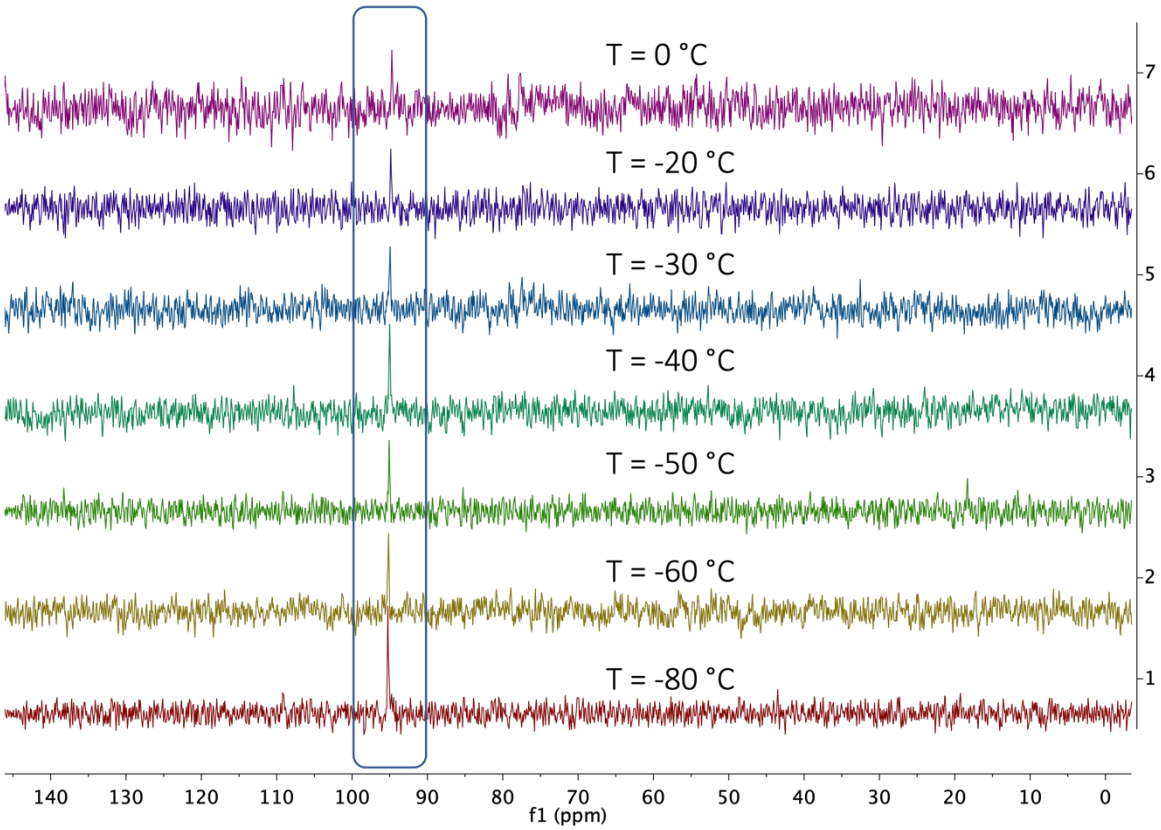

*Figure S20: Variable Temperature ^{31}P-NMR spectra of **4** between -80 and 0 °C in* n-hexane-d_{14}.

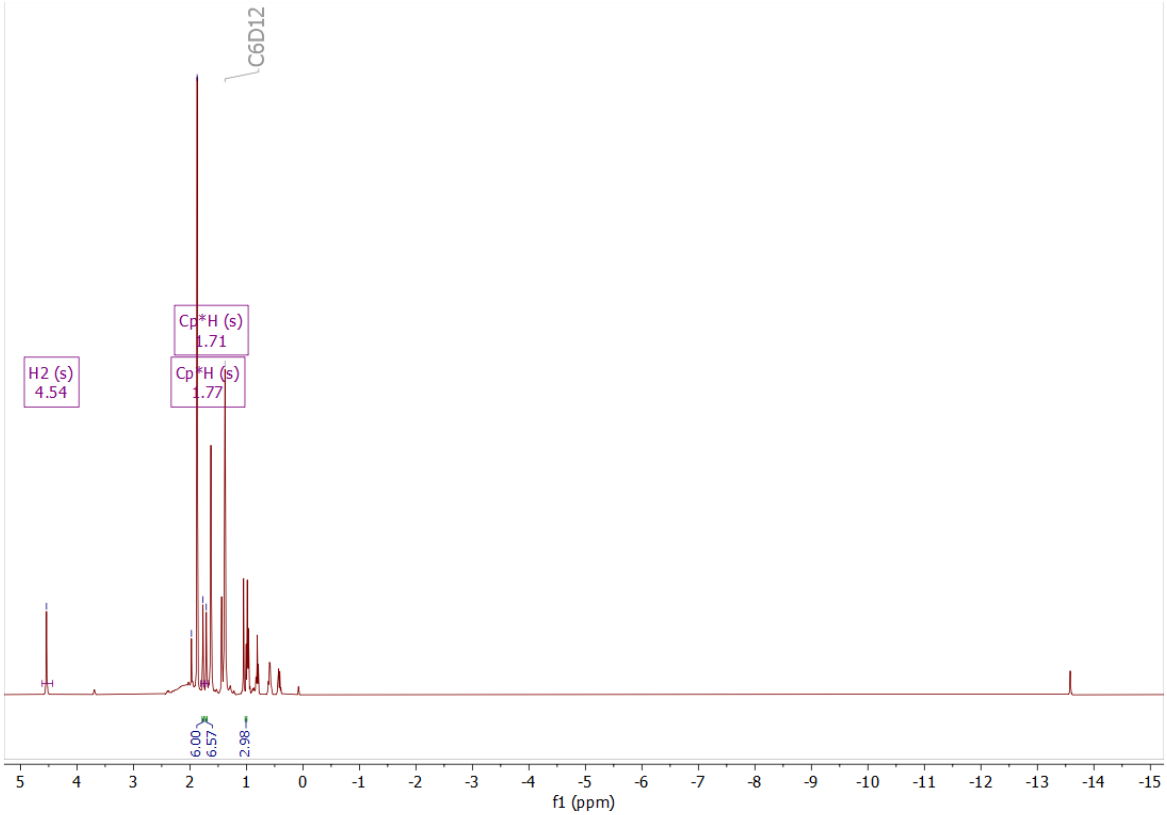

*Figure S21: ^{1}H NMR spectrum of the reaction of **1** with H_2 under 1 h irradiation (350 nm).*

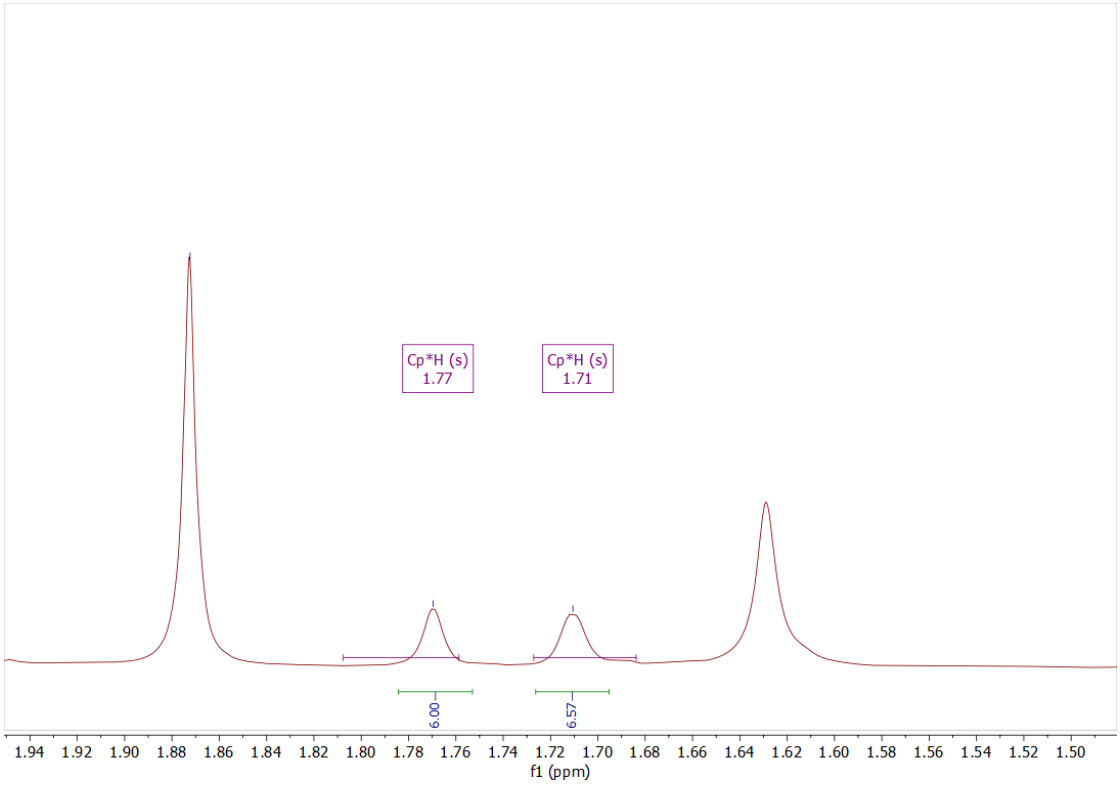

*Figure S22: Excerpt of ^{1}H NMR spectrum of the reaction of **1** with H_2 under 1 h irradiation (350 nm). Showing peaks of free Cp*H at 1.71 and 1.77 ppm.*

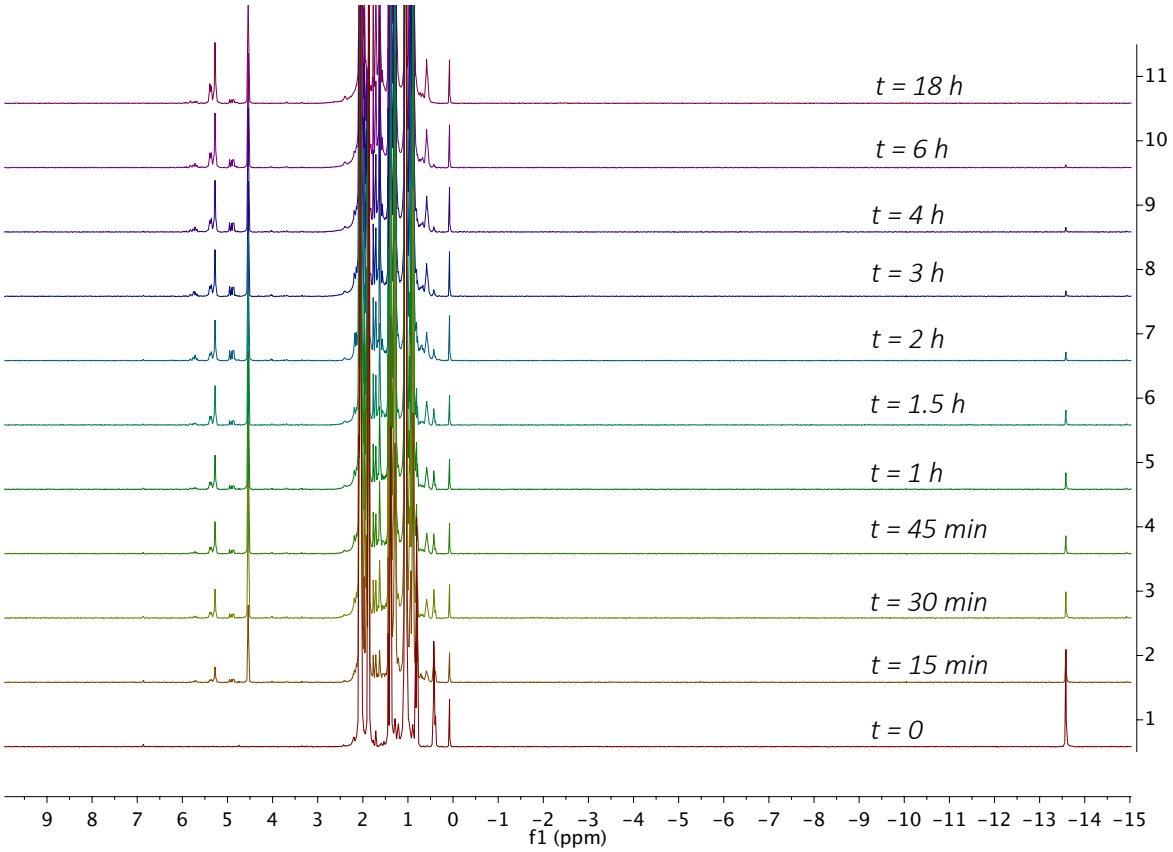

*Figure S23: Full range stacked ^{1}H NMR spectra of the conversion of 3-hexyne with **1** (5 mol%) under a dihydrogen atmosphere (2 bar) at 350 nm. Hydride shift of **1** at -13.6 ppm; alkenes and hydrosilylation products between 4.75 and 6.0 ppm.*

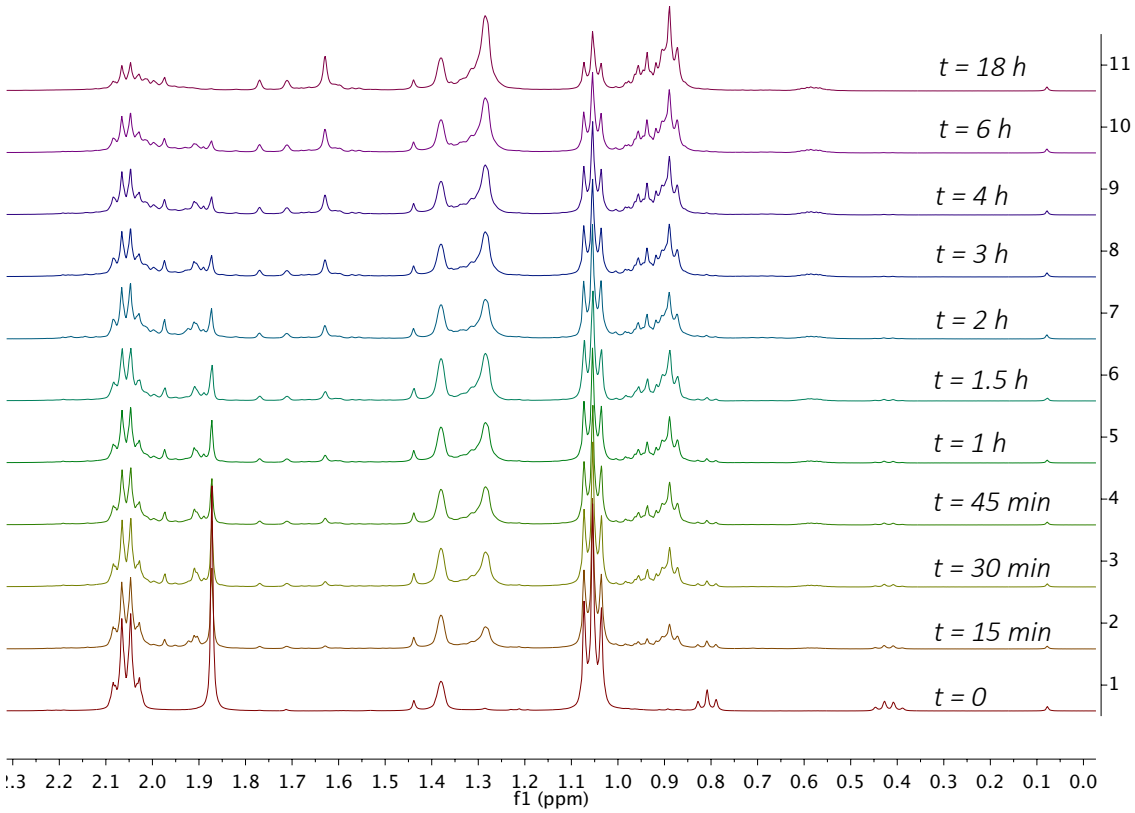

*Figure S24: Zoomed in stacked ^{1}H NMR spectra of the conversion of 3-hexyne with **1** (5 mol%) under a dihydrogen atmosphere (2 bar) at 350 nm. 3-Hexyne at 2.06 and 1.05 ppm; n-hexane (CH_2) between 1.20 and 1.36 ppm; CH_3 of n-hexane and hexenes between 0.85 and 1.01 ppm.*

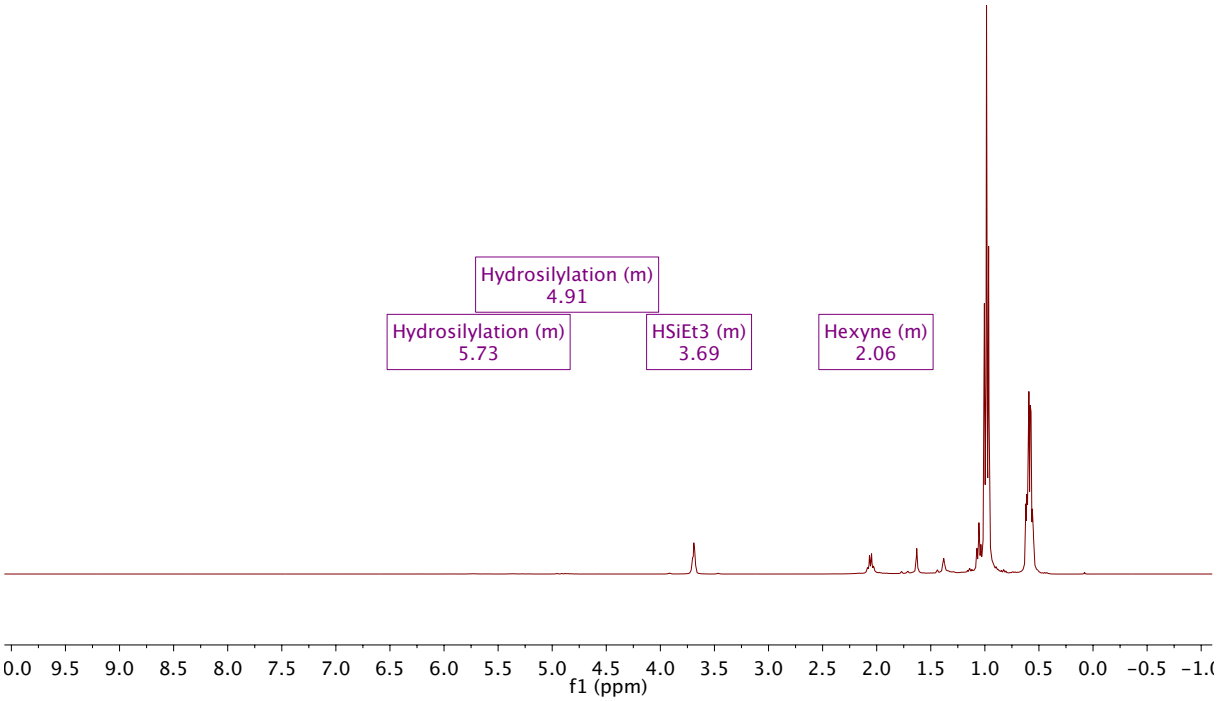

*Figure S25: Full range ^{1}H NMR spectrum of the conversion of 3-hexyne (1.0 eq.) and $HSiEt_3$ (5.0 eq.) with **1** (5 mol% against 3-hexyne) at 350 nm.*

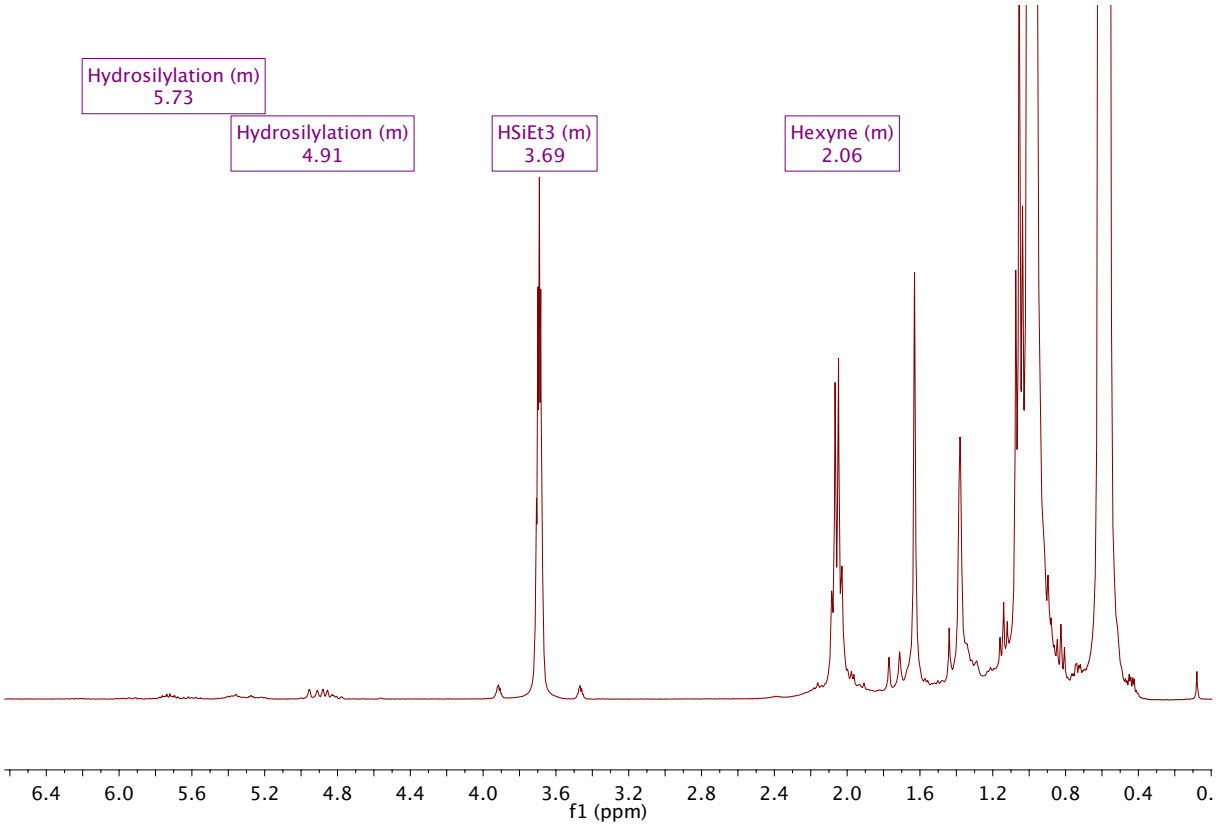

*Figure S26: Zoomed in ^{1}H NMR spectrum of the conversion of 3-hexyne (1.0 eq.) and $HSiEt_3$ (5.0 eq.) with **1** (5 mol% against 3-hexyne) at 350 nm.*

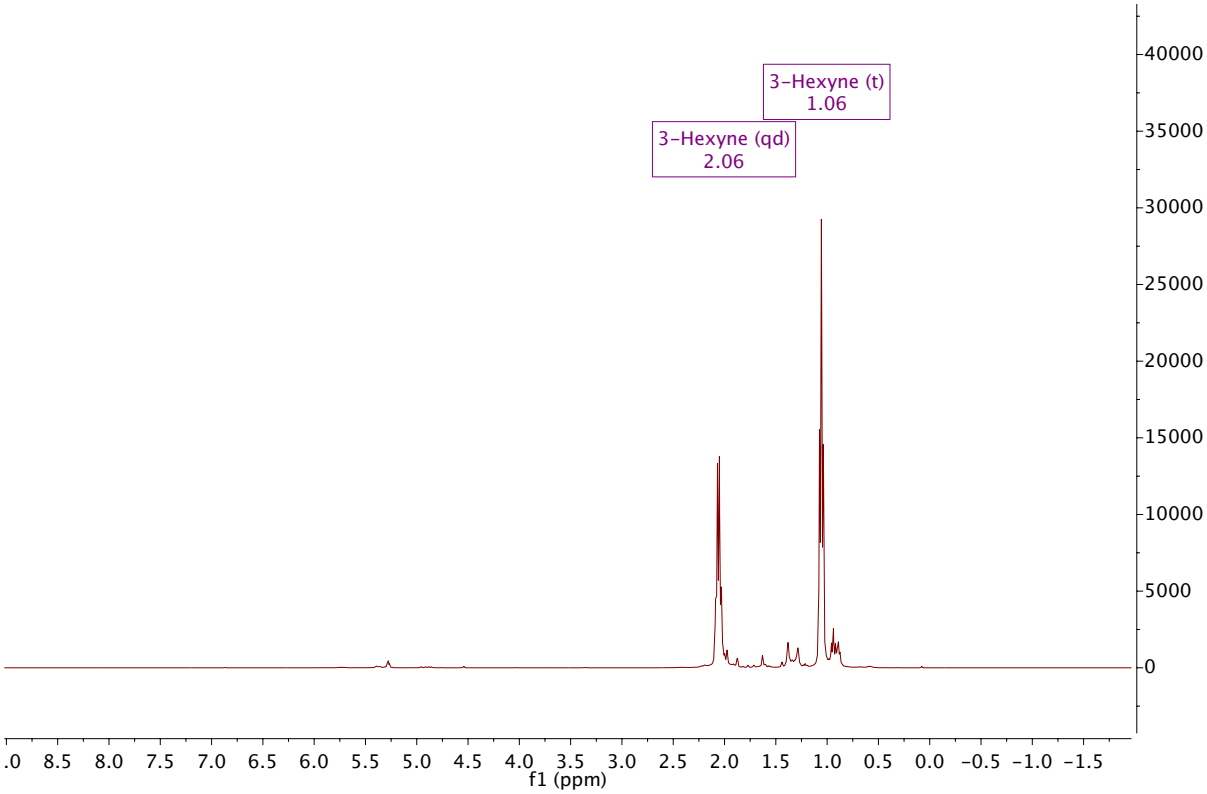

*Figure S27: Full range ^{1}H NMR spectra of the conversion of 3-hexyne with **1** (1 mol%) under a dihydrogen atmosphere (2 bar) after 24h at 350 nm.*

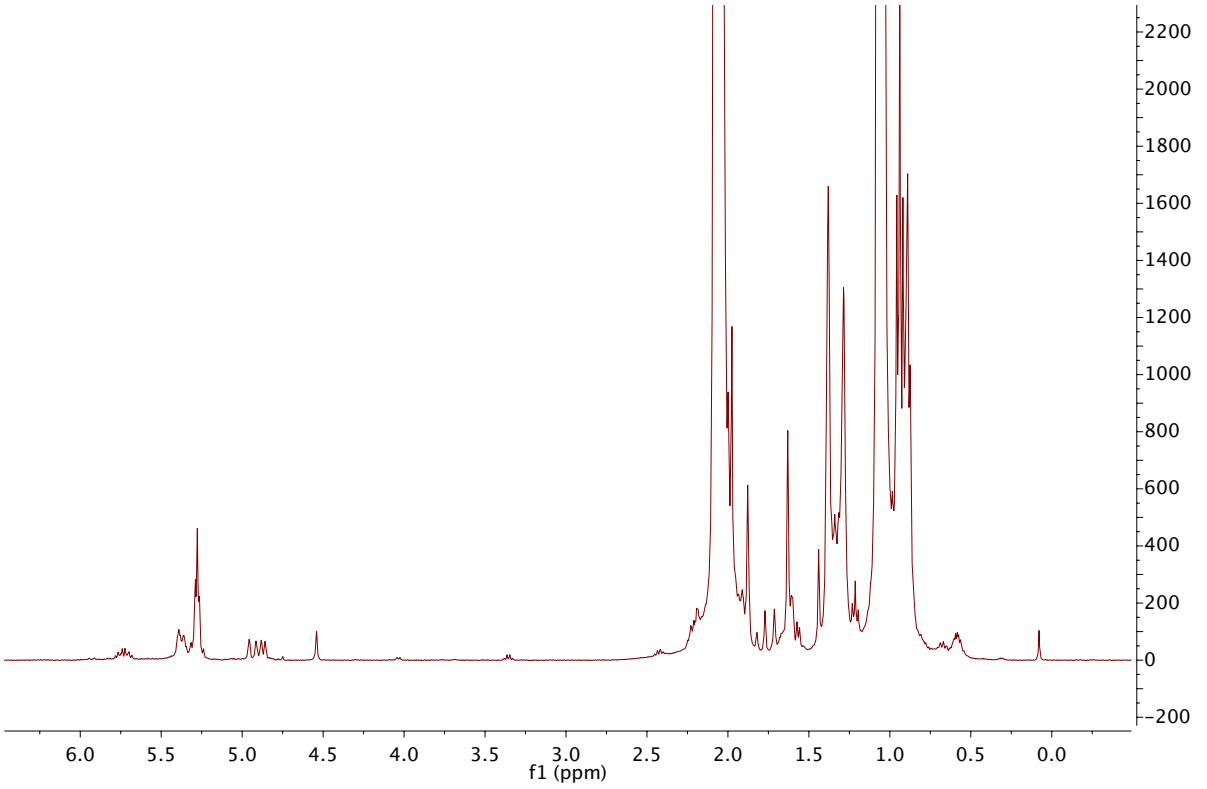

*Figure S28: Zoomed in ^{1}H NMR spectra of the conversion of 3-hexyne with **1** (1 mol%) under a dihydrogen atmosphere (2 bar) after 24h at 350 nm. Hexenes and hydrosilylation products between 4.75 and 6.0 ppm; n-hexane (CH_2) between 1.20 and 1.36 ppm; CH_3 of n-hexane and hexenes between 0.85 and 1.01 ppm.*

LIFDI mass spectra

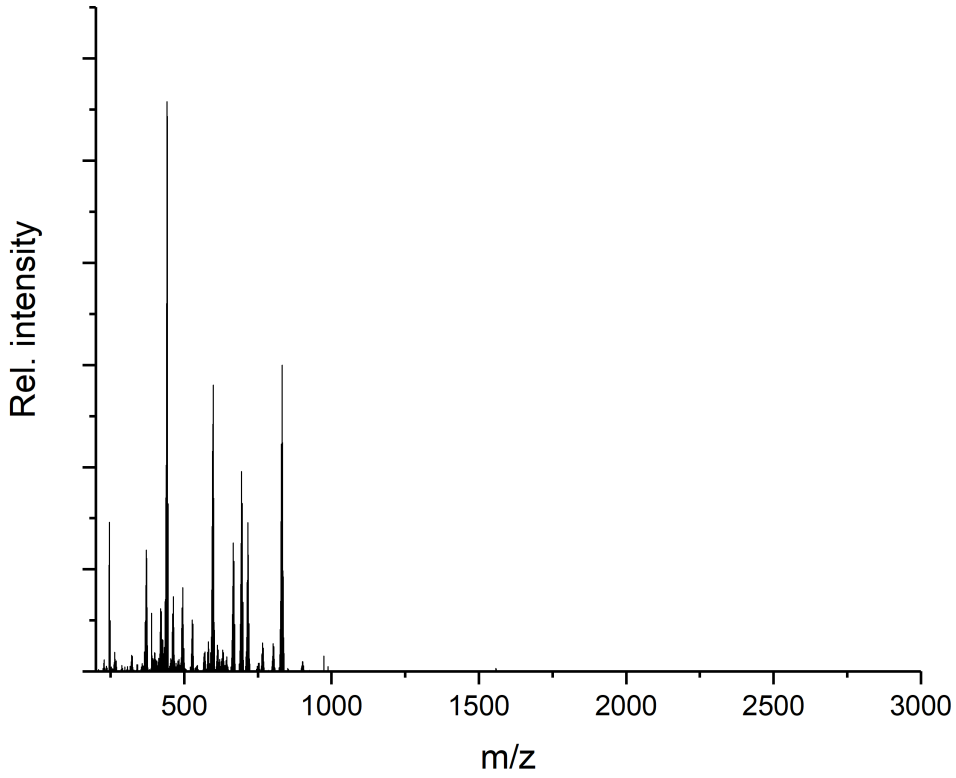

*Figure S29: LIFDI mass spectrum of **1** after 8 h irradiation in cyclohexane. Main pattern corresponds to **1** (m/z = 832.13) $[M-2H]^+$.*

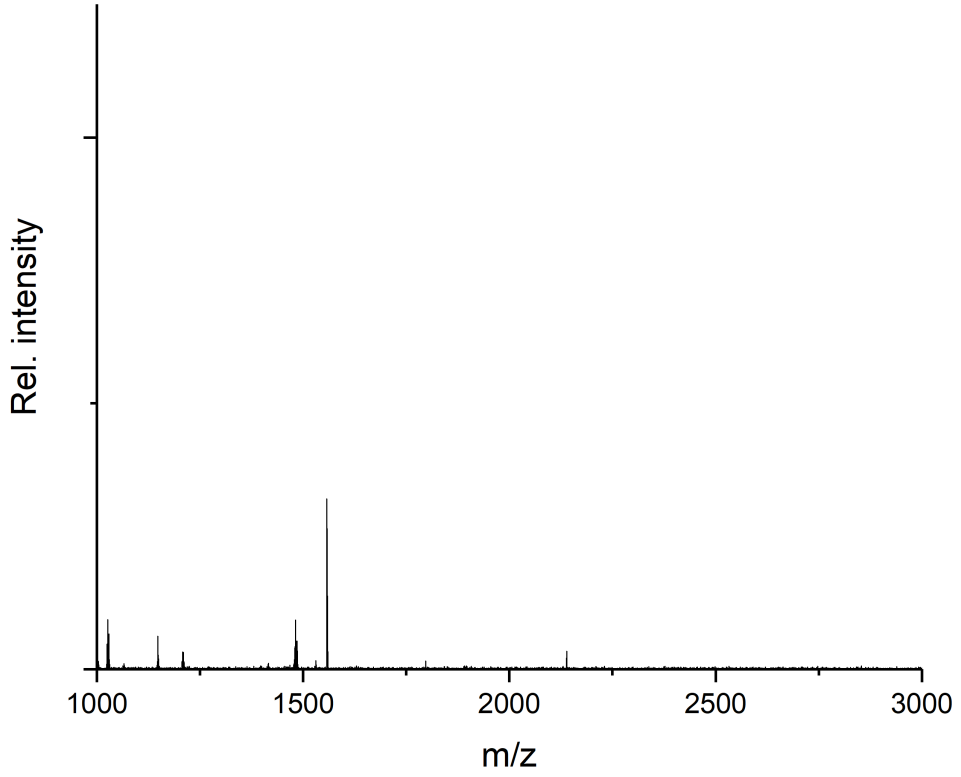

*Figure S30: Excerpt of LIFDI mass spectrum of **1** after 8 h irradiation in cyclohexane. No peaks at higher masses – barely any cluster growth visible.*

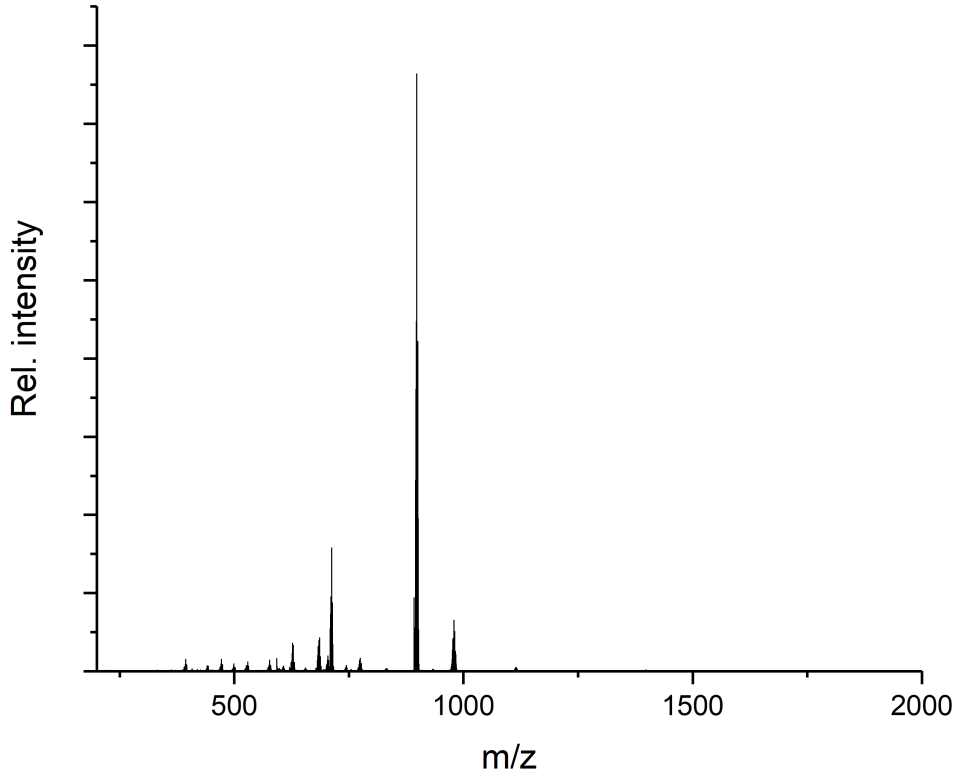

Figure S31: LIFDI mass spectrum of [(dppe)Ru(GaCp)$_3$]* ***4****. [M]$^+$ (m/z =* 1114.1656; calc. 1114.1671); [M-Cp*]$^+$ *(m/z =* 979.0478; calc. 979.0497); [M-2Cp*-Ga]$^+$ *(m/z =* 775.0068; calc. 775.0080). Main peak at *m/z =* 898.1727 attributed to *[Ru(dppe)$_2$]* (calc. 775.0080), formation assumed upon ionization.

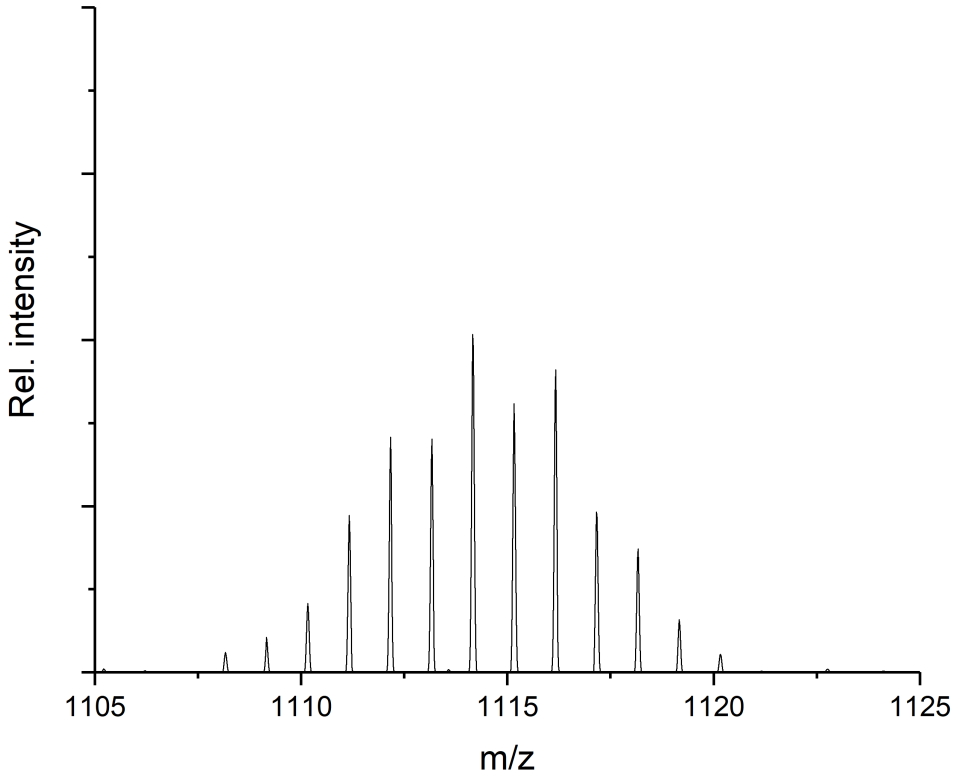

Figure S32: LIFDI mass spectrum of ***4****. Excerpt of isotopic pattern of* ***4****. [M]$^+$ (m/z =* 1114.1656; calc. 1114.1671).

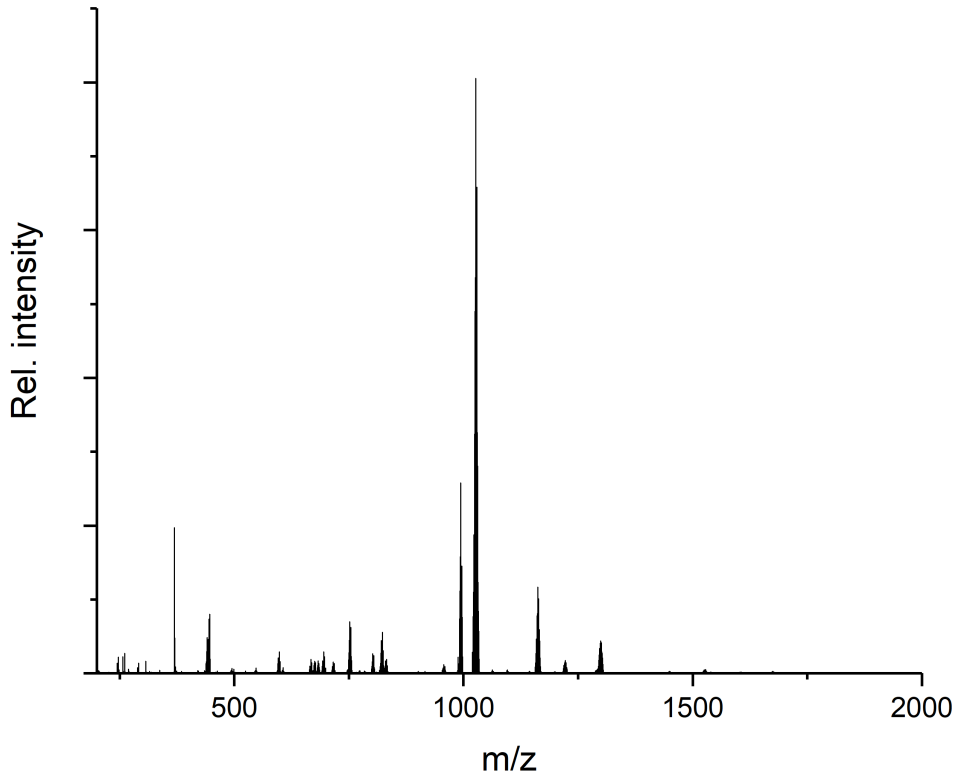

*Figure S33: In situ LIFDI mass spectrum of the reaction **1** with 1 eq 1,2-bis(diphenylphosphino)benzene after 24 h irradiation (350 nm).*

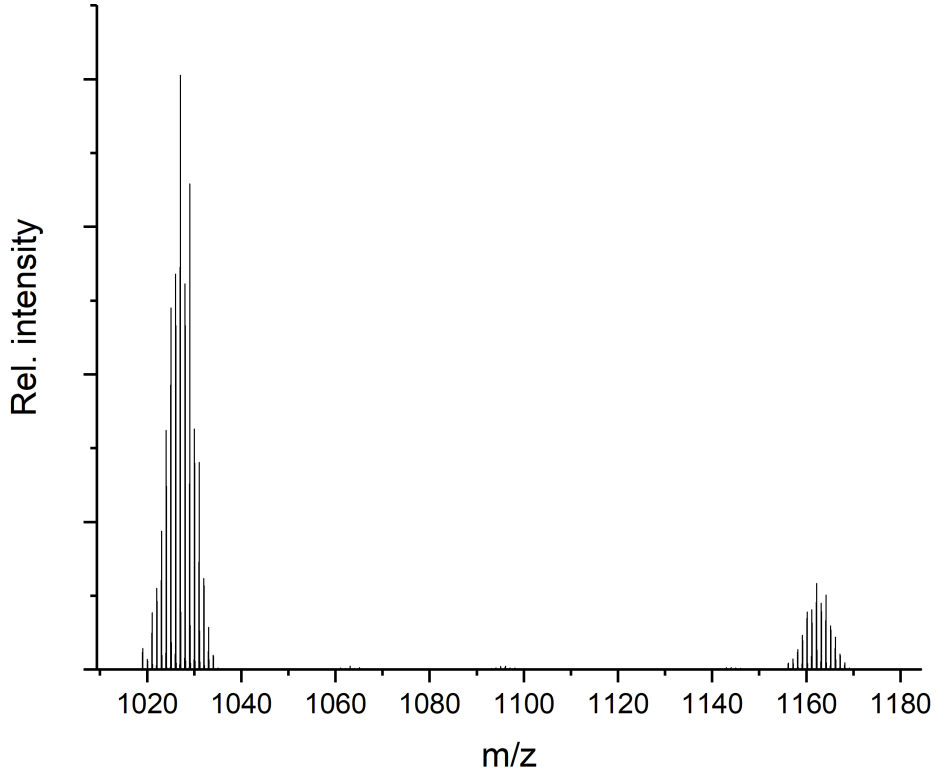

*Figure S34: Excerpt of LIFDI mass spectrum of the reaction **1** with 1 eq 1,2-bis(diphenylphosphino)benzene (dppbz) after 24 h irradiation (350 nm). Peaks assigned to: m/z = 1162.18 $[(dppbz)Ru(GaCp^*)_3]^+$ (calc. 1162.17); m/z = 1027.05 $[M\text{-}Cp^*]^+$ (calc. 1027.05).*

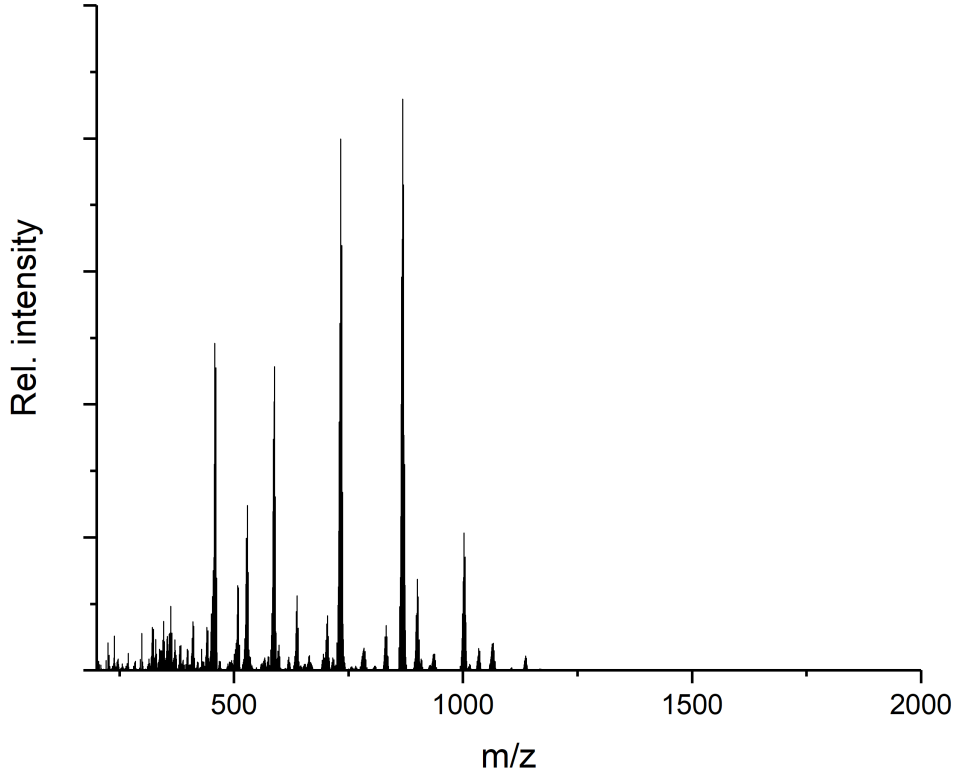

*Figure S35: In situ LIFDI mass spectrum of the reaction **1** with 2 eq trimethyl phosphine after 24 h irradiation (350 nm).*

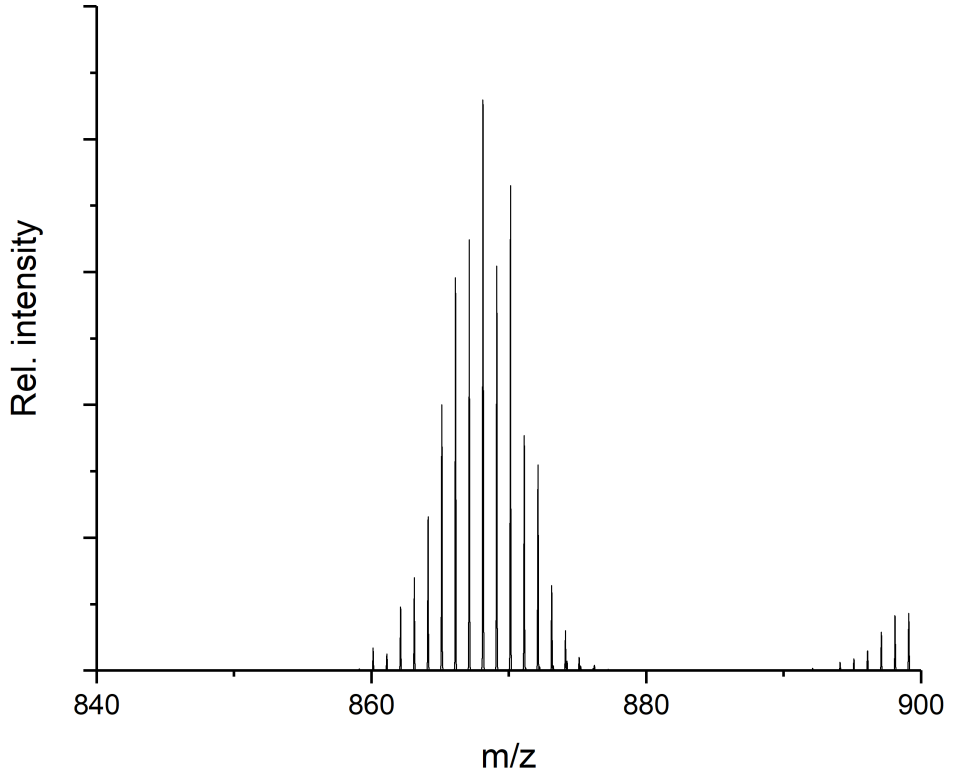

*Figure S36: Excerpt of LIFDI mass spectrum of the reaction **1** with 2 eq trimethyl phosphine (PMe_3) after 24 h irradiation (350 nm). Peak assigned to: m/z = 868.1195 $[(Me_3P)_2Ru(GaCp^*)_3]^+$ (calc. 868.1202).*

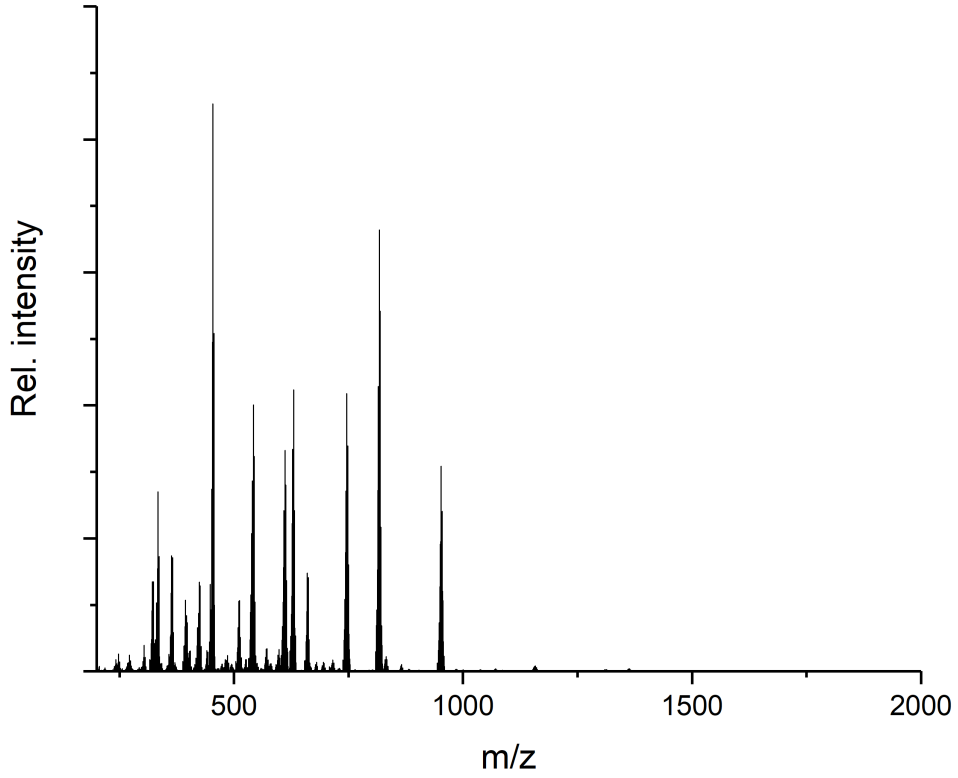

*Figure S37: In situ LIFDI mass spectrum of the reaction **1** with 2 eq triethyl phosphine after 24 h irradiation (350 nm).*

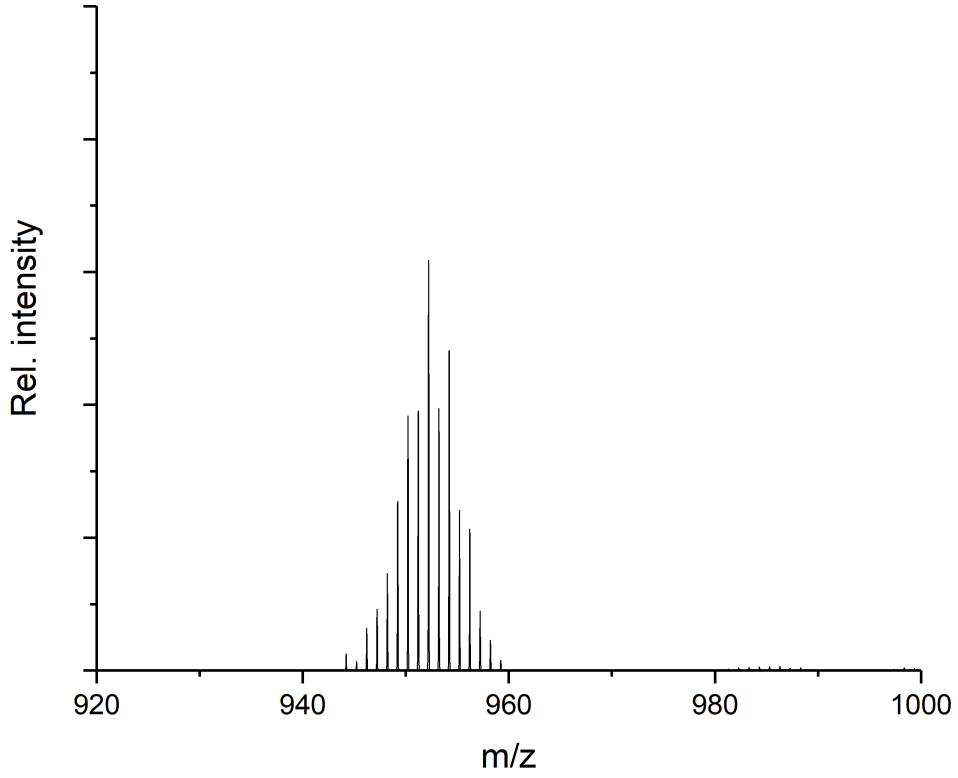

*Figure S38: Excerpt of LIFDI mass spectrum of the reaction **1** with 2 eq triethyl phosphine (PEt_3) after 24 h irradiation (350 nm). Peak assigned to: m/z = 952.2143 $[(Et_3P)_2Ru(GaCp^*)_3]^+$ (calc. 952.2141).*

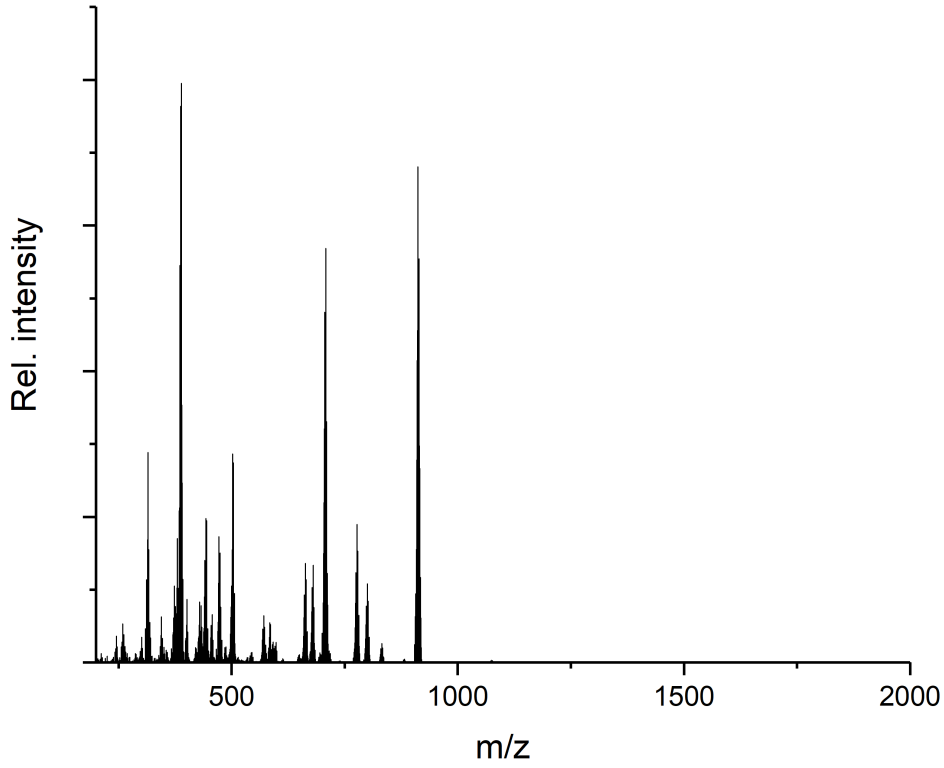

Figure S39: In-situ LIFDI mass spectrum of catalytic hydrogenation of 20 eq 3-hexyne under irradiation.

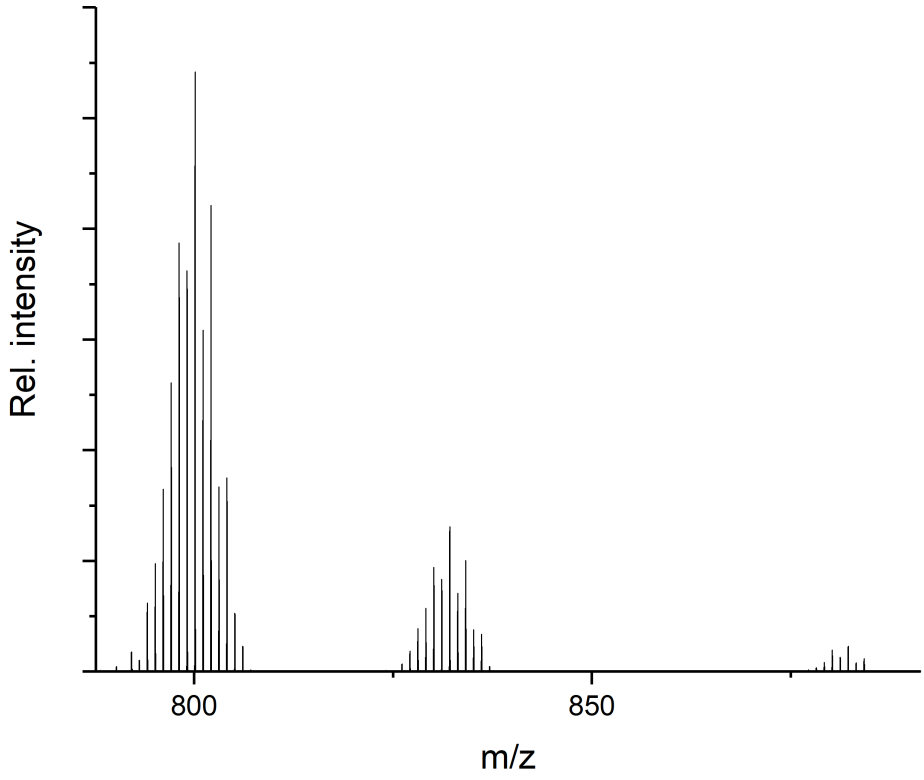

Figure S40: Excerpt of in-situ LIFDI mass spectrum of catalytic hydrogenation of 20 eq 3-hexyne under irradiation. Peak attributed to [Ru(GaCp)$_3$(hexene)] (**A$_2$**; m/z = 800.1251; calc. 800.1257) significantly more intense than peak attributed to [Ru(GaCp*)$_3$(hexyne)(hexene)] (**B**; m/z = 882.2044; calc. 882.2039). Inverse to reaction with higher 3-hexyne concentration. Peak at m/z = 832 results from unconverted **1**.*

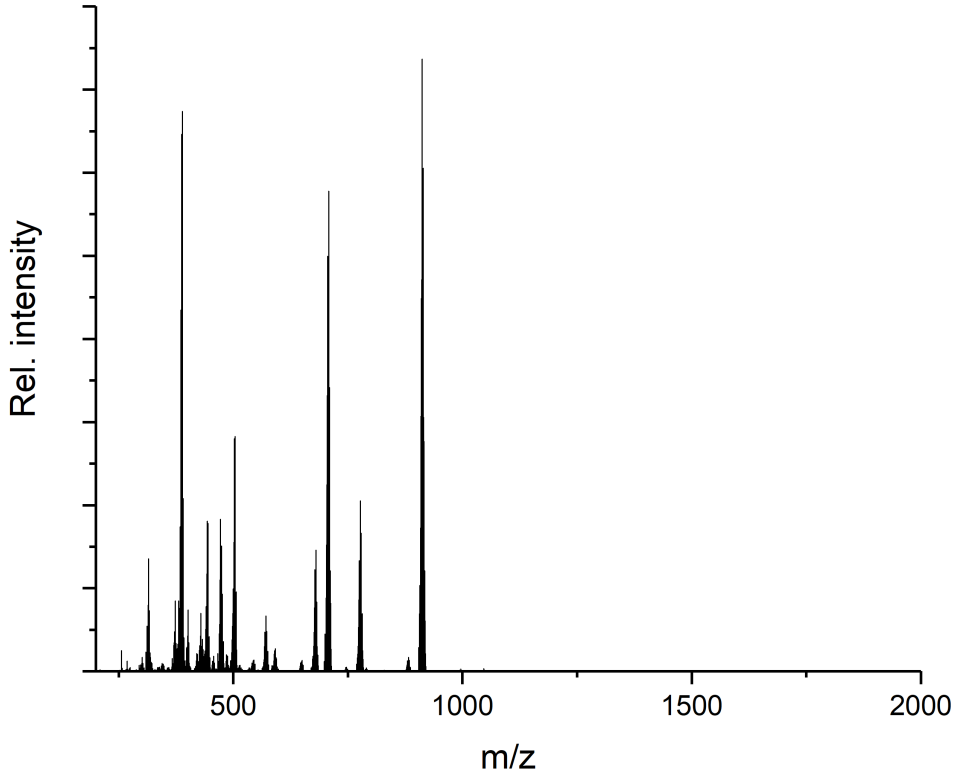

Figure S41: In-situ LIFDI mass spectrum of catalytic hydrogenation of 100 eq 3-hexyne under irradiation.

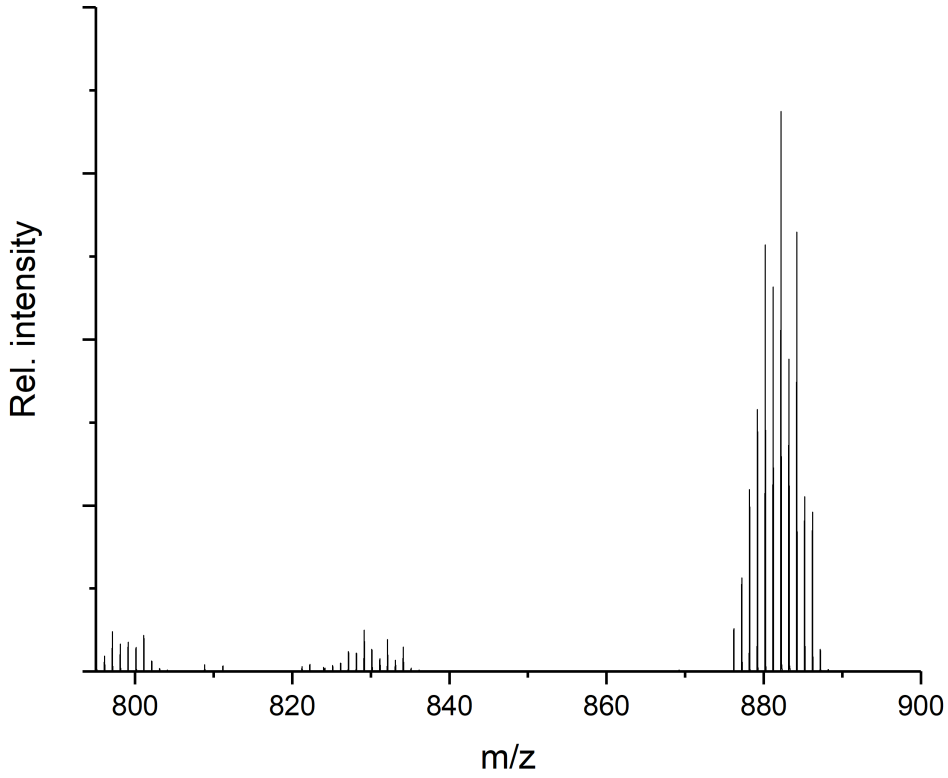

Figure S42: Excerpt of in-situ LIFDI mass spectrum of catalytic hydrogenation of 100 eq 3-hexyne under irradiation. Peak attributed to [Ru(GaCp)$_3$(hexyne)(hexene)] (**B**; m/z = 882.1997; calc. 882.2039) significantly more intense than peak attributed to [Ru(GaCp*)$_3$(hexene)] (**A$_2$**; m/z = 800.1180; calc. 800.1257). Inverse to reaction with lower 3-hexyne concentration. Peak at m/z = 832 results from unconverted **1**.*

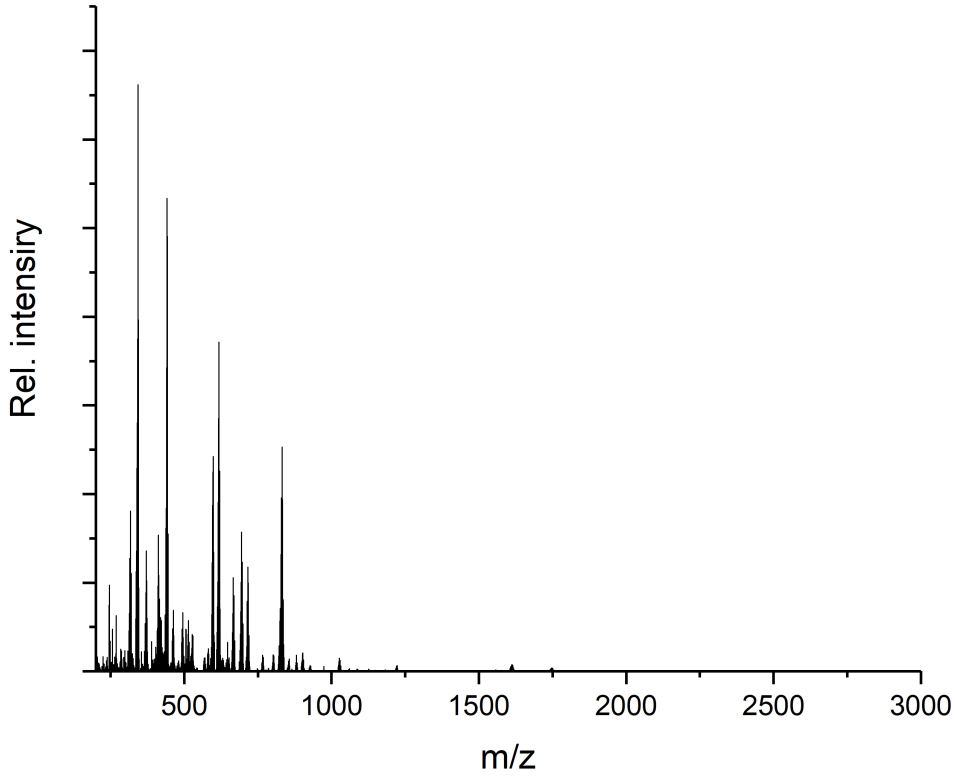

*Figure S43: LIFDI mass spectrum of the reaction of **1** with H_2 under 3 h irradiation (350 nm).*

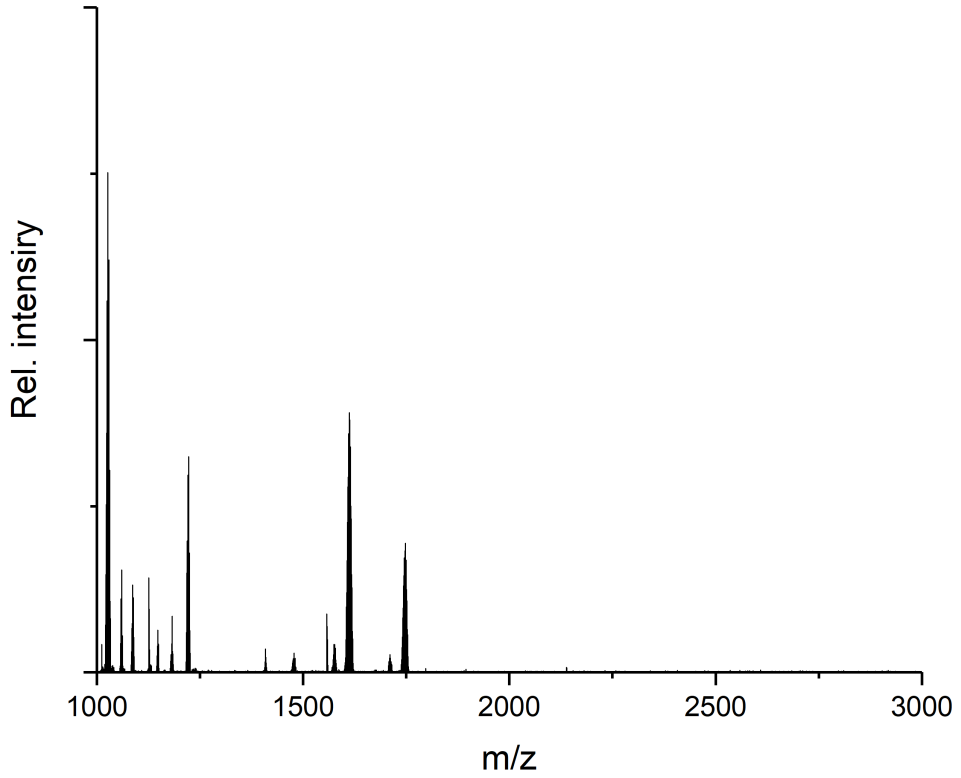

*Figure S44: Excerpt of LIFDI mass spectrum of the reaction of **1** with H_2 under 3 h irradiation (350 nm). Peaks assigned to composition as following: m/z = 1026.96 ($Ru_2Ga_4Cp^*_4H_5$), m/z = 1612.60 ($Ru_3Ga_9Cp^*_5H_5$), m/z = 1710.07 ($Ru_2Ga_8Cp^*_7H_3$) and m/z = 1747.73 ($Ru_3Ga_9Cp^*_6H_5$).*

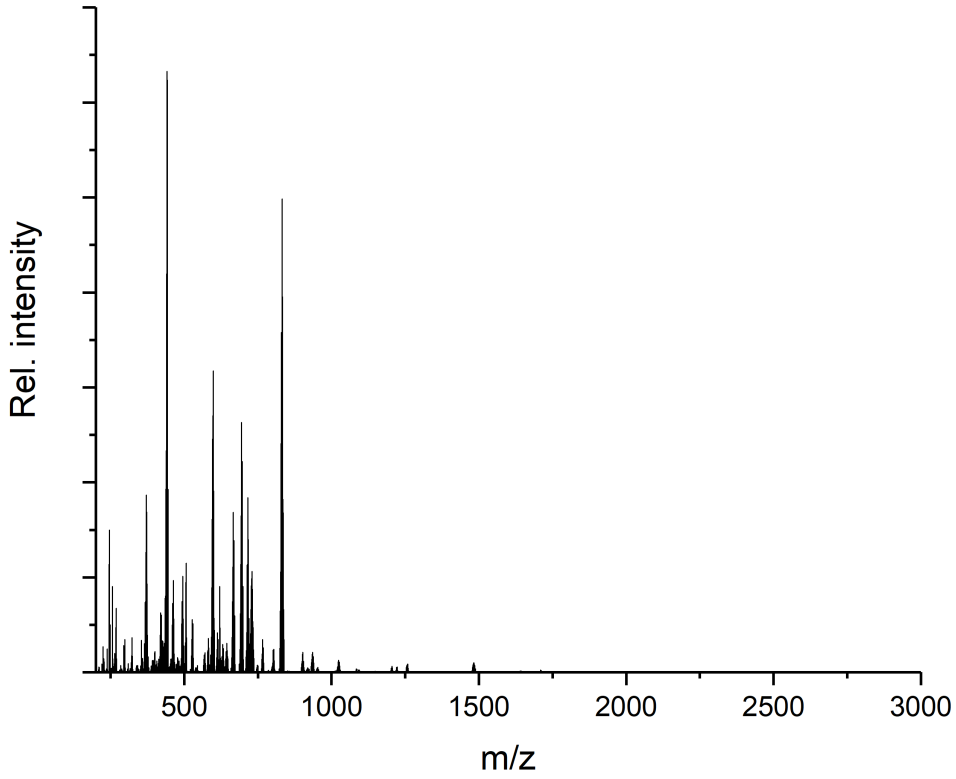

*Figure S45: LIFDI mass spectrum after the catalytic conversion 3-hexyne with **1** and H_2 (2 bar) under 24 h irradiation (350 nm) in cyclohexane-d_{12}.*

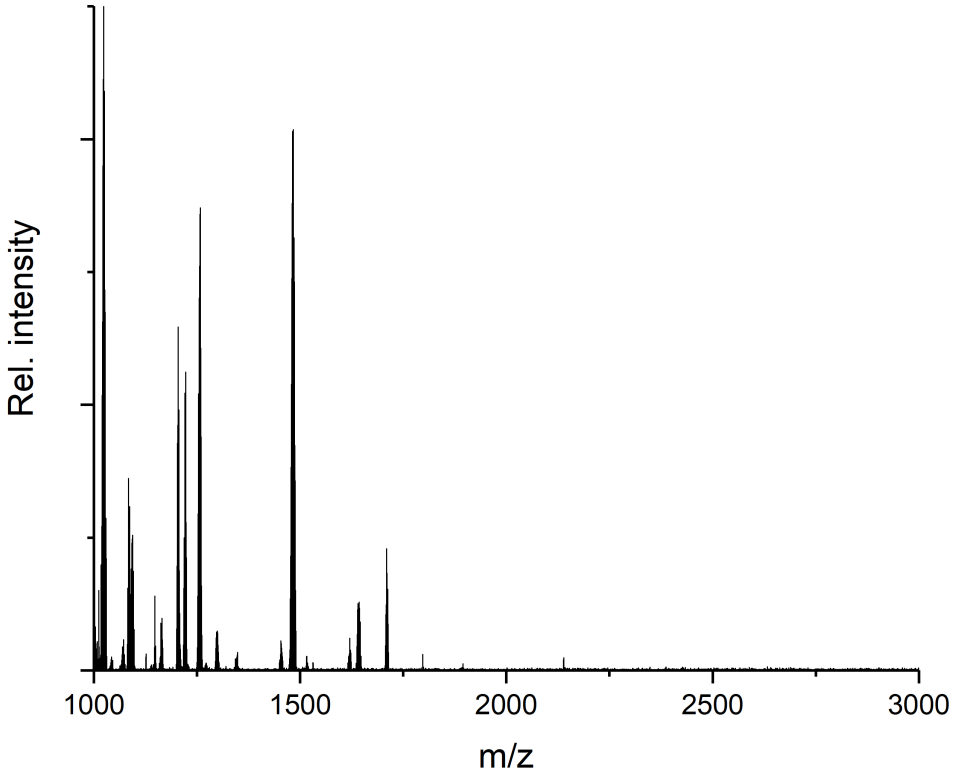

Figure S46: Excerpt of LIFDI mass spectrum after the catalysis. Several new clusters are formed: m/z = 1024.00 ($Ru_2Ga_4Cp^*_4H_2$); m/z = 1093.92 ($Ru_2Ga_5Cp^*_4H$); 1481.96 ($Ru_2Ga_7Cp^*_5SiEt_3H$); m/z = 1710.07 ($Ru_2Ga_8Cp^*_7H_3$).

IR spectra

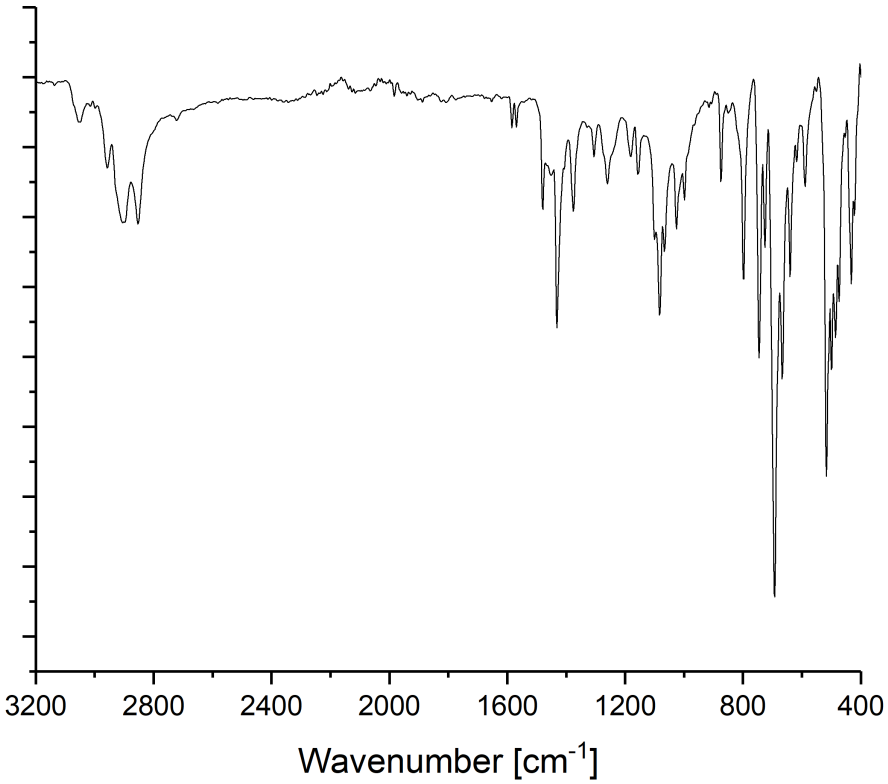

Figure S47: ATR-IR spectrum of [Ru(GaCp)$_3$(dppe)] (**4**). No typical Ru-H bands (range between 1600 and 2000 cm^{-1}).*

UV-Vis spectra

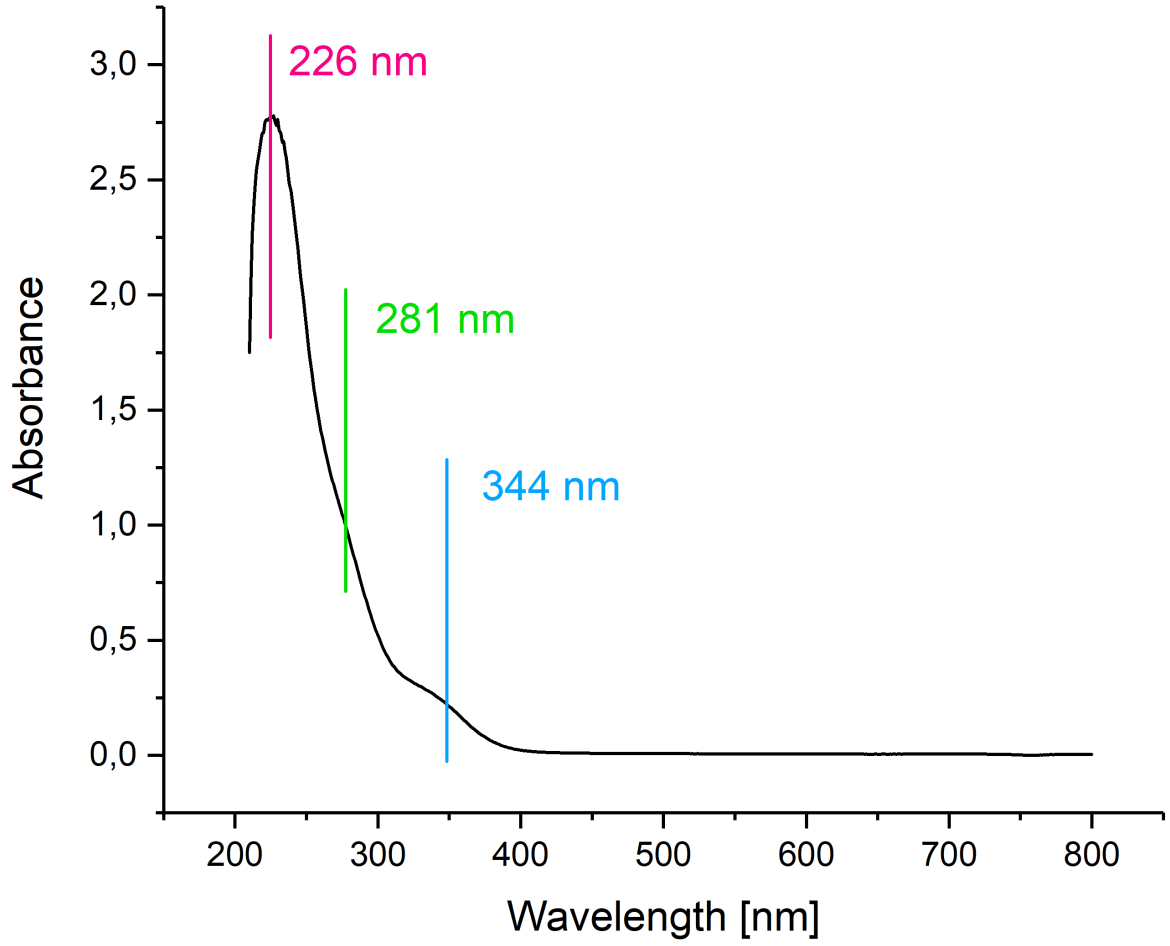

*Figure S48: UV-Vis of **1** in cyclohexane. Reprinted with permission.[S1]*